# THE SENTINEL LANDSLIDE

# ZION NATIONAL PARK,

# UTAH

by

Jessica J. Castleton

A thesis submitted to the faculty of
The University of Utah
in partial fulfillment of the requirements for the degree of

Master of Science

in

Geology

Department of Geology and Geophysics

The University of Utah

August 2015

Copyright © Jessica J. Castleton 2015

All Rights Reserved

The University of Utah Graduate School

STATEMENT OF THESIS APPROVAL

The thesis of **Jessica J. Castleton**

has been approved by the following supervisory committee members:

| | | |
|---|---|---|
| **Jeffrey Moore** | , Chair | **05/04/2015** <br> Date Approved |
| **Susan Ivy-Ochs** | , Member | Date Approved |
| **Paul Jewell** | , Member | **05/04/2015** <br> Date Approved |

The thesis has also been approved by **John Bartley**

Chair of the Department/College/School of **Geology and Geophysics**

and by David Kieda, Dean of The Graduate School.

ABSTRACT

The Sentinel rock avalanche in Zion National Park is one of the largest catastrophic landslide events recognized in the North American desert southwest. Originating from the western wall of Zion Canyon near its confluence with Pine Creek, the initial collapse removed a nearly 900 m high wall of predominantly Navajo sandstone. Energetic deposition is revealed by the relatively flat and hummocky topography of the debris field, which blocked flow of the Virgin River out of Zion Canyon. We combine new mapping of rock avalanche deposits with reconstruction of past topography to constrain the landslide extent, thickness, volume, and subsequent erosion. We estimate the original debris field covered an area of 3 million $m^2$, was ~3.3 km long where it blocked the Virgin River, and had a volume of 284 million $m^3$. The mean estimated thickness is 93 m, with a maximum deposit thickness of 200 m. Since deposition, erosion by the Virgin River has removed approximately 45%, or 131 million $m^3$ of the Sentinel rock avalanche debris. Cosmogenic nuclide surface exposure dating of 12 boulders from across the surface of the rock avalanche deposit reveals a mean age of $4.8 \pm 0.4$ ka. Results further show that boulders from across the slide were deposited simultaneously, indicating a single-event, massive and catastrophic failure scenario. Numerical simulation of rock avalanche runout was performed using the 'equivalent-fluid' code DAN3D, and the results show excellent match to our mapped deposit extents and estimated thickness. The simulated rock avalanche crossed Zion Canyon in

only ~20 s, with maximum velocities exceeding 90 m/s, ran up the opposing wall, and spread laterally up and down canyon. The Virgin River was dammed by landslide debris, which formed the extensive Sentinel Lake, eventually trapping a vast quantity of lacustrine and alluvial sediment. The cumulative effects reveal the long-lasting and diverse impacts of large rock avalanches in desert canyons of the Colorado Plateau: in addition to representing an extreme magnitude hazard, large landslides events also have wide-ranging ecological and geomorphic effects, here helping create the flat valley floor of Zion Canyon.

TABLE OF CONTENTS

LIST OF FIGURES

Figures

## ACKNOWLEDGEMENTS

I would like to thank Dr. Jeff Moore for his patience and support in my pursuit of obtaining this master's degree. Thank you to Dr. Paul Jewell for agreeing to be on my committee. Thanks to Dr. Susan Ivy-Ochs at the laboratory for Ion Beam Physics at ETH Zurich for hosting me and allowing me to use the laboratory to date the samples. While preparing the samples in the lab, I could not have done so without the help from Christian Wirsig and Michael Rüttimann. Thank you for teaching me the process and helping out with preparation. Special thanks to Nuria Casacuberta for saving my ability to sleep and my sanity while in Zurich and to all the rest at ETH who quickly became good friends. Thank you to Dave Sharrow with Zion National Park for his awesome support of this research by allowing us access to the park and contributing his distinctive knowledge of the rock avalanche and locations of geologic interest. I had a lot of help in the field, in particular from Greg McDonald, Tyler Knudsen, and Ali Sherman. Finally, thank you Scott, Justin, and Mark for helping me in the field, letting me be absent for chunks of time, and always supporting me in everything I do.

# 1. INTRODUCTION

## 1.1 Mass Wasting Hazards

Deserts of the American Southwest are a geologically dynamic environment. The slow weathering of sandstone juxtaposed with rapid geologic processes, such as catastrophic landslides, shape the desert landscape into a beautiful, life-sustaining environment in which we recreate and increasingly develop. Wind, monsoonal rain, and frost action slowly erode and weather the exposed bedrock, while punctuated events such as floods, rock falls, and earthquakes have shaped the landscape in significant ways. The accessible beauty of Zion Canyon is owed in part to one of the largest landslides known in the United States, the Sentinel rock avalanche. Also referred to as the Sand Bench Landslide, this massive rock avalanche (sensu Hungr et al., 2001) dammed the Virgin River, forming a lake (Grater, 1945; Hamilton, 1984), eventually filling Zion Canyon with sediment that creates the flat valley floor that makes this part of the canyon accessible.

Rock falls and rock slides are common occurrences in the deserts of the American southwest. Large-scale mass wasting events, while infrequent, have the potential to affect large areas and can have catastrophic consequences (Crosta et al., 2007; Pankow et al., 2014). However, the mechanism, frequency, volume, and mechanics of rock avalanches in southern Utah are not well documented and understood. In a more general sense, catastrophic mass wasting events, such as rock avalanches and gravity-driven slides, in arid environments remain poorly understood due to limited identification and mapping, leading to undocumented modern examples, poorly constrained prehistoric case histories, and limited application of direct investigational approaches (Friedmann, 1997).

## 1.2 Objectives of Study

Rock avalanches are generally understudied outside of alpine environments. In a region such as Zion National Park with increasing development prospects and high tourism traffic, an understanding of rock avalanche mechanisms and frequencies is paramount. Comprehensive geological-engineering investigation and direct dating are here used to describe key parameters of catastrophic mass wasting for the Sentinel landslide, and to explore subsequent geomorphic and anthropogenic impacts.

With a pre-investigation estimated volume in the range of 200-300 million $m^3$, the Sentinel rock avalanche is roughly five times larger than the largest historical landslide in North America (Pankow et al., 2014). A modern event of this magnitude would have devastating effects in Zion National Park or surrounding communities. This investigation aims to obtain a direct age of the event using cosmogenic nuclide surface exposure dating, accurately calculate the volume of the rock avalanche, and conduct runout analysis based on reconstruction of pre-failure topography to explore plausible failure scenarios. Crucial questions to be addressed are when the Sentinel slide occurred, what mechanism of failure initiated the slide, whether it was a single event or multiple events, and what the implications are for catastrophic landslide events in Zion National Park.

## 1.3 Background

The first geologist (Grater, 1945) to map and describe the Sentinel rock avalanche deposit did so out of interest in investigating smaller-scale slides that frequently originate from the larger landslide body, which have blocked the Virgin River in the past and caused destruction of Zion Canyon Scenic Drive (Figure 1). Grater (1945) studied destructive landslide events that occurred in 1923 and again in 1941, mapped the prehistoric rock avalanche, and estimated the potential lake extent. The Sentinel rock avalanche deposit remains a problem for the park with continued sloughing and occasional large landslides. In 1995, a landslide occurred from the eastern slope where incised by the Virgin River (Sharrow, 1995). The landslide dammed the river, forming a pond that reached 6 m depth before the river was able to cut through the blockage (Solomon, 1995; Schuster and Wieczorek, 1995). There is no canyon outlet north of the Sentinel debris; therefore, landslides that dam the river, and block the road have the potential to trap visitors and employees in Zion Canyon. Continual repairs to infrastructure have been necessary, and the threat to people and property downstream remains as landslides continue to occur from the incised Sentinel rock avalanche debris.

Theories for the source area and failure mechanism of the Sentinel slide have been presented by Hamilton (2014; 1976) and Biek et al. (2012; 2004). Hamilton described the rock avalanche as a large mass that broke away from the western wall of Zion Canyon and slumped to the valley floor as a coherent block, or so-called Toreva. First described by Reiche (1937), a Toreva Block refers to “a landslide consisting essentially of a single large mass of unjostled material which, during descent, has under-gone a backward rotation toward the parent cliff about a horizontal axis which roughly parallels it.” Toreva Block topography consists of cliff forming sandstone underlain by weaker materials.

Biek et al. (2012; 2004) proposed an alternative explanation to the Toreva Block mechanism, involving the collapse of a narrow wall or fin of Navajo Sandstone. The hypothesized wall/fin would have separated the main Zion Canyon from a tributary canyon that ran roughly parallel to the west, following joints in the Navajo Sandstone. The wall/fin was thought to have collapsed as the Virgin River and tributary to the west cut into the Kayenta formation at its toe.

Three previous radiocarbon dates indicate that Sentinel Lake filled the valley between ~8000 and 4000 years B.P. (Biek et. al., 2004). Two dates from charcoal in lacustrine sediment sampled near the base of a drill hole by the Utah Geological Survey gave ages of 8009 ± 844 calendar years and 7651 ± 570 calendar years B.P., though in incorrect stratigraphic succession (Utah Geological Survey personal communication). These radiocarbon ages were interpreted to indicate that the lake was present by at least 6200 to 8000 years B.P. (Biek et al., 2003). Radiocarbon dating performed on charcoal in sandy deltaic deposits near the northern end of the slide yielded a calendar age of 3930 ± 525 years B.P. (Hamilton, 1976; 1984). Radiocarbon dating, however, provides an indirect method for obtaining the age of a landslide. No prior investigations have attempted to date the rock avalanche deposits directly.

A recent optically stimulated luminescence (OSL) date taken from a sand layer interbedded within lacustrine clay deposits at an elevation of 1312 m gave an age of 4.31 ± 1.3 ka B.P. (Hamilton, 2014). Together, the $^{14}C$ and OSL ages have been interpreted to indicate that Sentinel Lake filled with sediment approximately 4000 years ago, and occupied the valley behind the landslide dam for ~4000 years (~8000 to 4000 years B.P.). Estimates indicate the Virgin River has eroded through 60 m of lake sediments, but that it still has to cut through approximately 20 m of landslide deposits before it re-establishes its pre-landslide gradient (Biek et al., 2003; Graham, 2006).

Lake deposits elsewhere in Zion National Park and the Springdale area have been mapped extensively, and indicate the repeated occurrence of large valley-blocking landslides (Hamilton, 2014; Lund et al., 2010). Lake formation has also been attributed to prehistoric basalt flows blocking major drainages (Knudsen and Lund, 2013).


**Figure 1.** Aerial view of Sentinel slide in 1945 (Grater, 1945). The deposit is outlined in red and the slide debris is labeled in the bottom center of the picture.

# 2. GEOLOGIC AND PHYSIOGRAPHIC SETTING

## 2.1 Study Area

Zion National Park consists of widely inaccessible, rugged terrain, dominated by sheer cliffs, hanging valleys, slot canyons, and unique ecosystems. Incorporating 368 square km (Graham, 2006), the park is located in southwestern Utah 495 km from Salt Lake City and 257 km from Las Vegas (Figure 2). To preserve the natural splendor, the area including Zion Canyon was first designated Mukuntuweap National Monument in 1909 (Knudesen et al., 2009). President Woodrow Wilson signed a bill that officially entered Zion National Park into the National Park system on November 20, 1919 (Taylor, 2008). The city of Springdale, located at the southern entrance of the park, with a population of 529, welcomes nearly 3 million tourists each year (NPS, 2014).

Zion Canyon has a rich cultural history. Water is the common theme that has drawn people into the harsh environment within the tight canyon walls. As early as 750 A.D., the earliest inhabitants were the Virgin Branch of the Ancestral Puebloan culture, formerly called the Virgin Anasazi, and the Parowan Fremont culture (Graham, 2006). Both cultures left evidence of their presence until the dramatic climate shift of the Little Ice Age, around 1200 A.D., dried the land and these agricultural peoples abandoned the canyon (Graham, 2006). Soon after, the Paiute people settled in Zion Canyon and the surrounding areas. Mormon pioneers began to explore and settle the area in the 1850s (Lund et al., 2010). Agriculture ceased when Zion was declared a national monument.

Artifacts of human occupation remain today as a tribute to catastrophic geologic processes shaping the land in ways that ultimately contributed to making it habitable.

## 2.2 Geologic Setting

Zion National Park is situated on the western margin of the Colorado Plateau near the transition with the Basin and Range province (Biek et al., 2003). From north to south, rocks become progressively older and are revealed in impressive canyons by the rapid downcutting of streams and rivers.

Bounded by the Hurricane fault zone to the west and the Sevier fault zone to the east (Biek et al., 2012), Zion National Park sits within a relatively undeformed crustal block (Rogers and Engelder, 2004). The sedimentary strata are nearly horizontal, with a slight regional dip to the east from 1-5° (Grater, 1945; Knudsen and Lund, 2013). Preferential erosion has created regularly spaced NNW-trending slot canyons that formed in along pre-existing joint zones in the Navajo Sandstone (Rogers and Engelder, 2004) (Figure 3).

The Hurricane fault is a large normal-slip fault. The fault is nearly 257 km long, making it the longest normal fault in southwestern Utah (Knudsen and Lund, 2013). Fault investigations indicate that the Hurricane fault produced several large-magnitudesurface-rupturing earthquakes in the late Quaternary. Paleoseismic investigations indicate that the fault can produce earthquakes in excess of magnitude 7 (Lund et al., 2007). Significant seismic events can contribute to the occurrence of landslides on multiple scales. Catastrophic rock avalanches are frequently triggered by large seismic events, and in some cases can be used as a proxy for strong ground motion typically occurring with a surface fault rupturing event (Barth, 2013). The Sentinel rock avalanche has not been correlated with a known paleoseismic event.

Detrital sedimentary rocks of Jurassic age comprise the Sentinel slide. The towering Sentinel peak is capped by the Sinawava member of the Temple Cap Formation, a reddish brown to dark red interbedded, fine-grained sandstone, silty sandstone and mudstone that was deposited in a coastal sabkha and tidal flat environment (Doelling et al., 2002; Biek et al., 2003). The white Navajo, just below the J-1 unconformity (Pipiringos and O'Sullivan, 1978) and underlying the Temple Cap, is light gray or white. Below, the more resistant reddish brown Pink Navajo forms ledges and benches. The ledges and crags of the lower Brown Navajo transition into the underlying Kayenta Formation. Before the vast deserts that created the Navajo, the Kayenta Formation was deposited in mudflats and fluvial environments at the transition zone where rivers flowed over a playa (Biek et al., 2000; Doelling et al., 2002. The reddish brown/reddish orange siltstone and fine-grained sandstone (Doelling et al., 2002) forming the steep slope of the Tenney Canyon Tongue of the Kayenta Formation comprises the upper third of the Kayenta (Biek et al., 2000). The dark red/brown siltstone and sandstone of the main body of the Kayenta forms steep slopes and ledges. The eolian Lamb Point Tongue of Navajo Sandstone pinches in and out within the Kayenta Formation. This reddish brown, cross-bedded, quartzose sandstone forms prominent cliffs. Deposited in a fluvial environment, the Springdale Member of the Moenave Formation forms a vertical cliff below the Kayenta (Doelling et al., 2002). Exposed below the southern portion of Sentinel rock avalanche, the Whitmore Point and the Dinosaur Canyon Members of the Moenave are not thought to be involved in the rock avalanche.

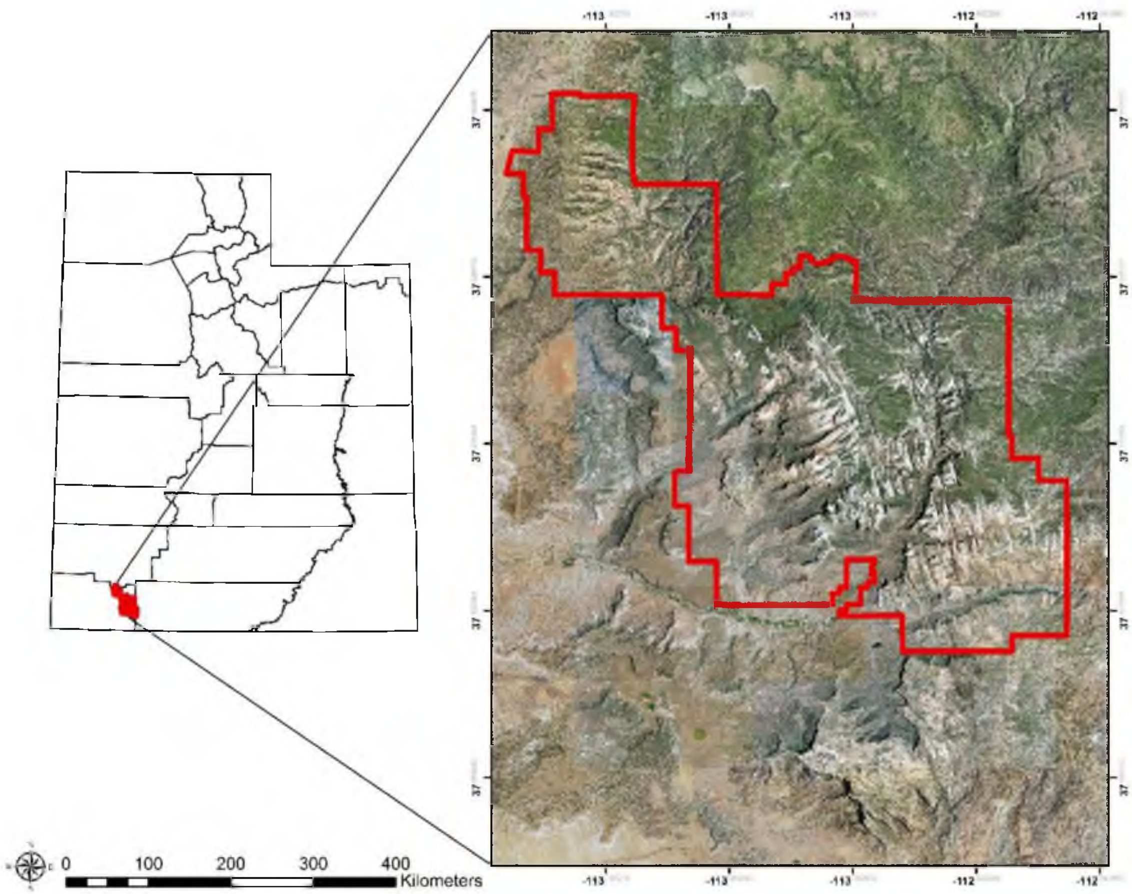


**Figure 2.** Location of Zion National Park in southwestern Utah.

**Figure 3.** Deep fractures, joints, and slot canyons in the Navajo Sandstone.

# 3. SENTINEL ROCK AVALANCHE

## 3.1 Geologic Mapping

Detailed geologic mapping was performed at a scale of 1:12,000 (Figures 4a and 4b). The body of the rock avalanche, original extent, and source area were mapped incorporating field reconnaissance, Digital Elevation Model (DEM) analysis, aerial photograph interpretation, and through the creation of eighteen cross sections detailing pre- and post-failure topography. The surrounding geology was mapped by Doelling et al. (2002); geologic mapping for this project, with the exception of the slide body, slide extent, and source area, was modified from this mapping.

The rock avalanche primarily involves the Navajo and Kayenta Formations, deposited on an apparently in-place ledge of the Springdale member of the Moenave Formation visible in the southern portion of the deposit area. Virgin River erosion reveals the internal structure of the rock avalanche where highly deformed and fractured Navajo and Kayenta is visible (Figure 5). The Whitmore Point Member and the Dinosaur Canyon Member of the Moenave Formation were identified and mapped on the east side of the Virgin River and the east side of Scenic Drive in the southern extent of the rock avalanche. The source area is identifiable by a ragged Navajo Sandstone cliff (Figure 6). The original estimated rock avalanche deposit is 3.3 km long from north to south and 1.4

km wide from west to east. Debris dammed the Virgin River forming Sentinel Lake, and also would have dammed adjoining Pine Creek (Figure 7).

## 3.2 Pre-failure Topography

Essential to investigation of the landslide is accurate representation of the pre-slide topography and failure surface, as well as the slide surface immediately after failure, which together can be used to generate an estimate of slide volume. Creation of topographic models was performed through field mapping, cross sections, and GIS modeling.

Pre-failure topographic modeling was conducted using a 10-m DEM, topographic cross sections, and geologic mapping combined in ArcGIS. Five cross sections (N1, N2, C, S7, S8; see Appendix A), three longitudinal sections for elevation control, and a long-profile of the Virgin River were generated for recreation of Zion Canyon topography before failure and beneath slide deposits. Seven cross sections (S1-S6 and C) and two longitudinal cross sections for elevation control were generated for recreation of the source area (Figure 8).

Differential erosion in the Jurassic sediments forms highly varied topography. Cross sections were drafted to estimate pre-failure and immediate post-failure topography (Figure 9 and Appendix A). A profile of the Virgin River from the Narrows to the East Fork was drafted to estimate the thickness of the rock avalanche deposit at each cross section (Figure 10).

Existing erosional surface angles and geomorphology were modified and adjusted to infer realistic release area and pre-failure canyon topography. Grids were created from topographic cross sections including pre-failure elevations and coordinate information. The topographic models created in this process were then used for volume analysis and runout modeling.

## 3.3 Volume Analysis

Pre-failure topographic analysis for the deposit and source area were used to determine the area, average and maximum thickness, and the volume of the Sentinel rock avalanche deposit. The final volume calculation should show good agreement between source and deposit, while accounting for bulking as intact rock is converted to debris; a bulking factor of 20-30% is typical (Hunger and Evans, 2004). The parameters of the source and deposit are provided in Table 1. To calculate the volume of the rock avalanche deposit, basal topography was subtracted from the post-failure topography using the cut-fill tool in ArcGIS. To calculate the volume of the source area, the post-failure topography was subtracted from the modelled pre-failure topography.

We determined that the original volume of the Sentinel slide deposit was 284 million $m^3$. This value is presumed accurate to within ±10% based on alternative trial solutions. Reconstruction of past topography and field mapping indicated an average thickness of 93 m (Figure 11). The area of the slide deposit was calculated to be approximately 3 million $m^2$. The unbulked source volume is 227 million $m^3$ and the maximum vertical thickness is 725 m (Figure 12). Subtracting the reconstructed post-slide surface from modern topography (Figure 13), the eroded volume was determined to be 131 million $m^3$, or roughly 45% of the original deposit. Some areas of added thickness occur in the region just below the current cliff face of the Sentinel, where a large talus sand cone (Qmts, Figure 4) consists of pulverized Navajo Sandstone from continued erosion of the cliff (Figure 14).

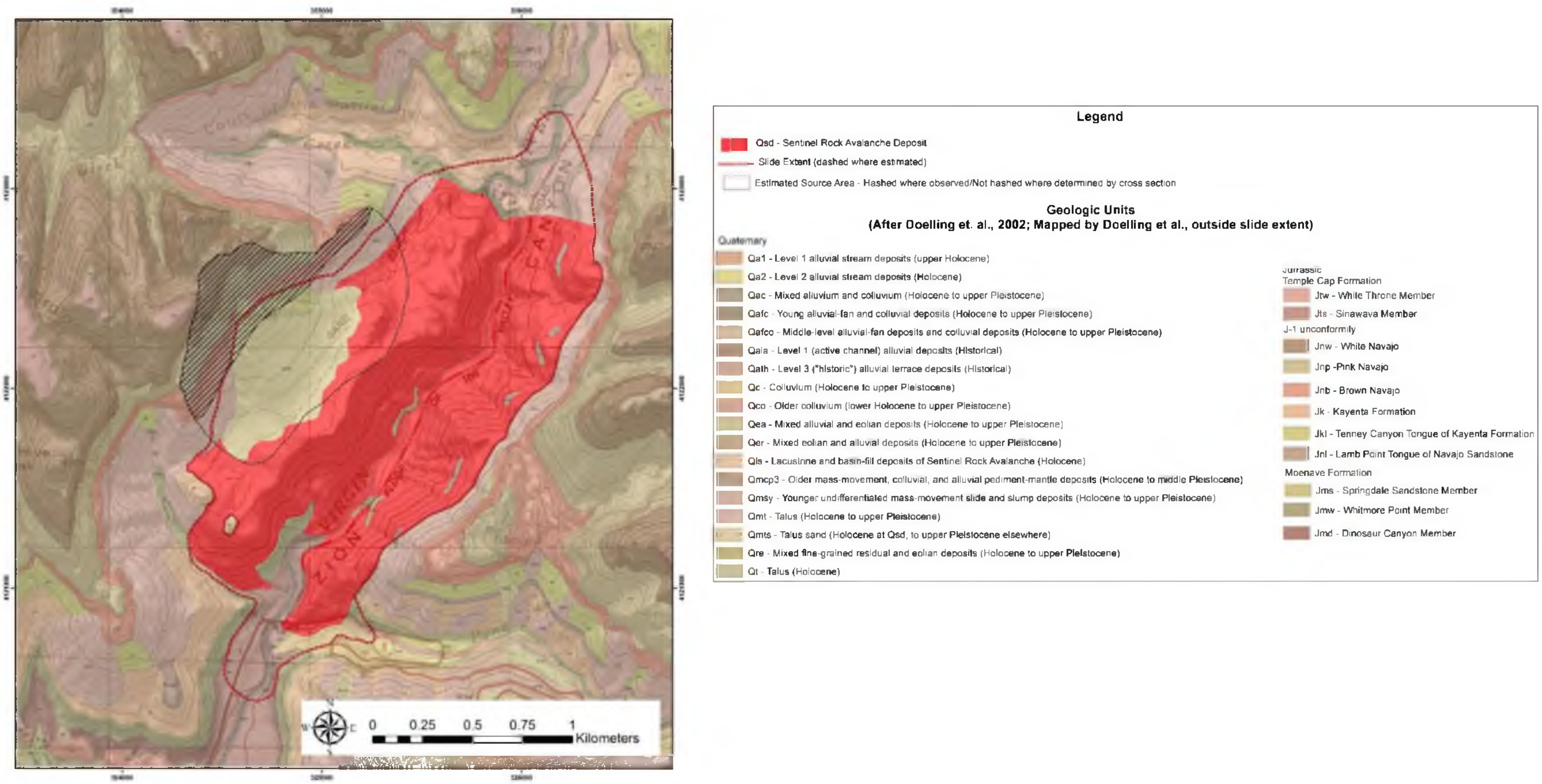


**Figure 4.** Geologic map of the Sentinel rock avalanche. Modified from Doelling et al., 2002.

**Figure 5.** Fractured Navajo Sandstone blocks in Sentinel rock avalanche debris.


**Figure 6.** Source area (outlined in red) of the Sentinel rock avalanche.

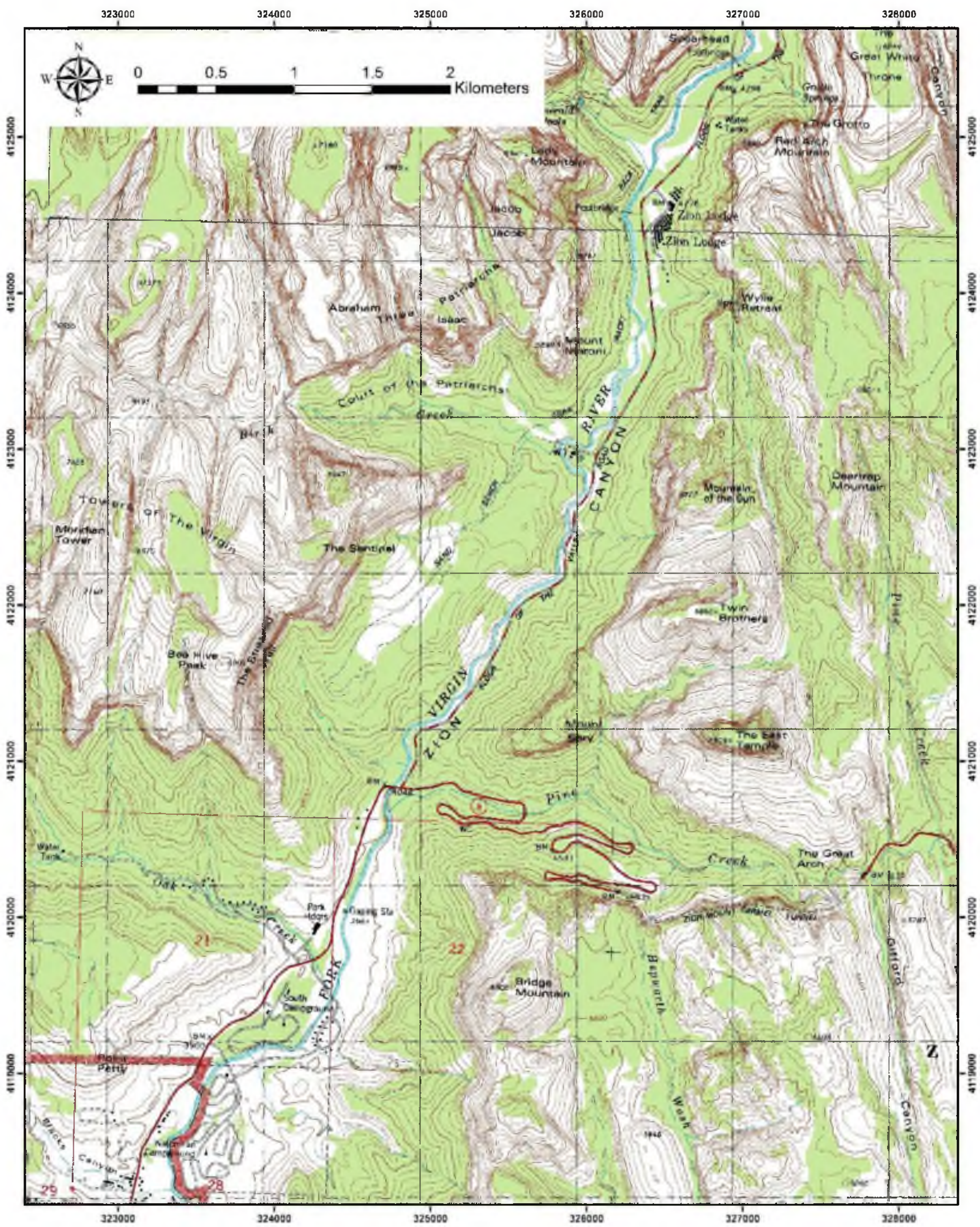


**Figure 7.** 1:24,000 topographic map showing area surrounding Sentinel rock avalanche (deposit outlined).

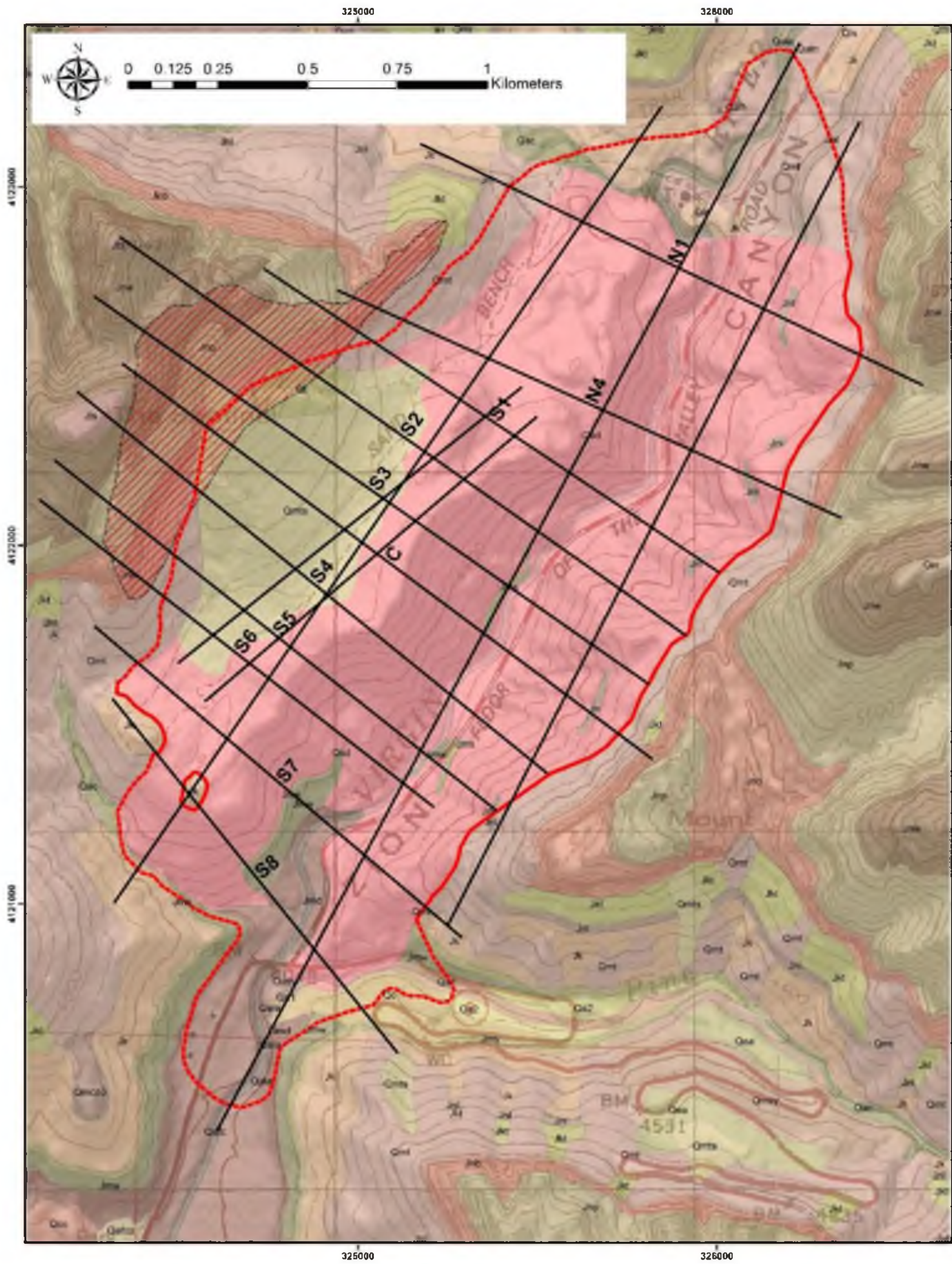


**Figure 8.** Location of cross sections used to develop elevation models in ArcGIS for use in volume calculations and runout modeling.

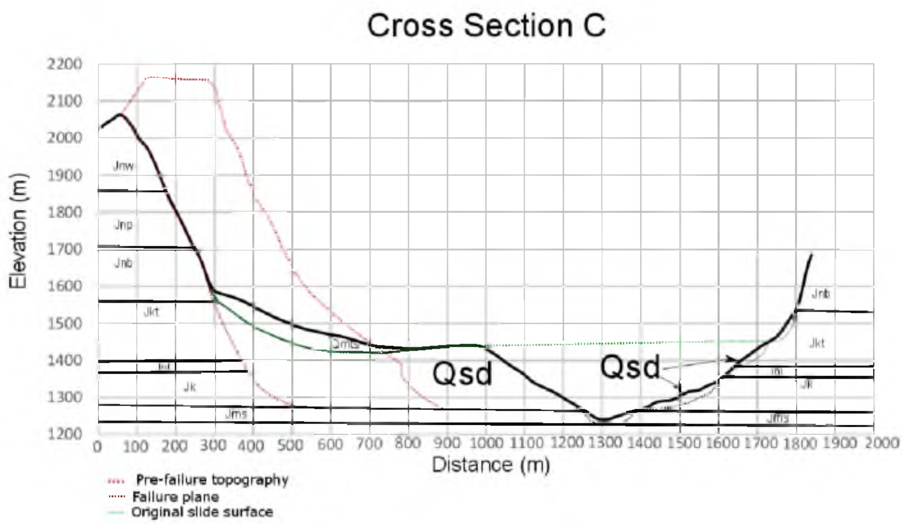


**Figure 9.** Example cross section. Cross section C was used for analysis of the bottom of the rock avalanche before failure, the top of the rock avalanche immediately after failure, and reconstruction of the source area. Additional cross sections are included in Appendix A.

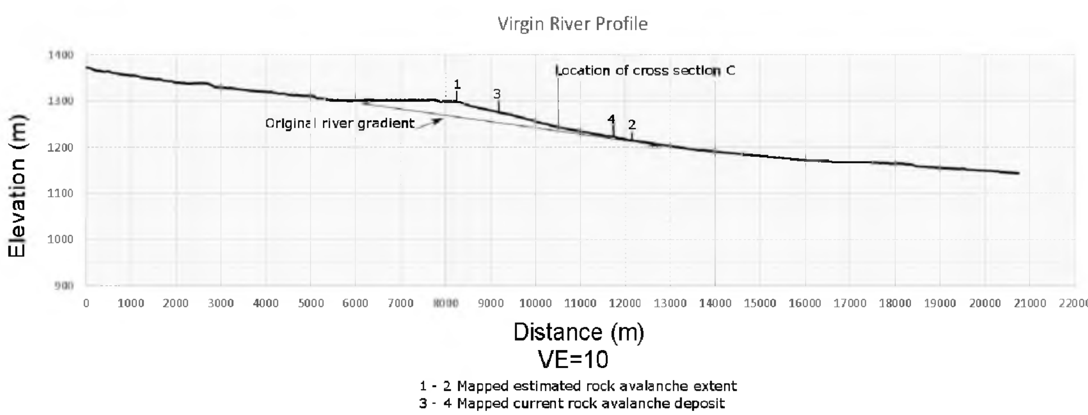


**Figure 10.** Longitudinal profile of the Virgin River from The Narrows to the East Fork of the Virgin River in Springdale.

**Table 1.** Parameters of the Sentinel rock avalanche deposit and source area.

| | Rock Avalanche Deposit | Source Area |
|---|---|---|
| Area ($m^2$) | 3,026,000 | 901,000 |
| Maximum Thickness (m) | 200 | 722 |
| Mean Thickness (m) | 93 | 315 |
| Volume ($m^3$) | 284,031,000 | 226,544,000 |
| Bulking Factor (%) | 28 | |

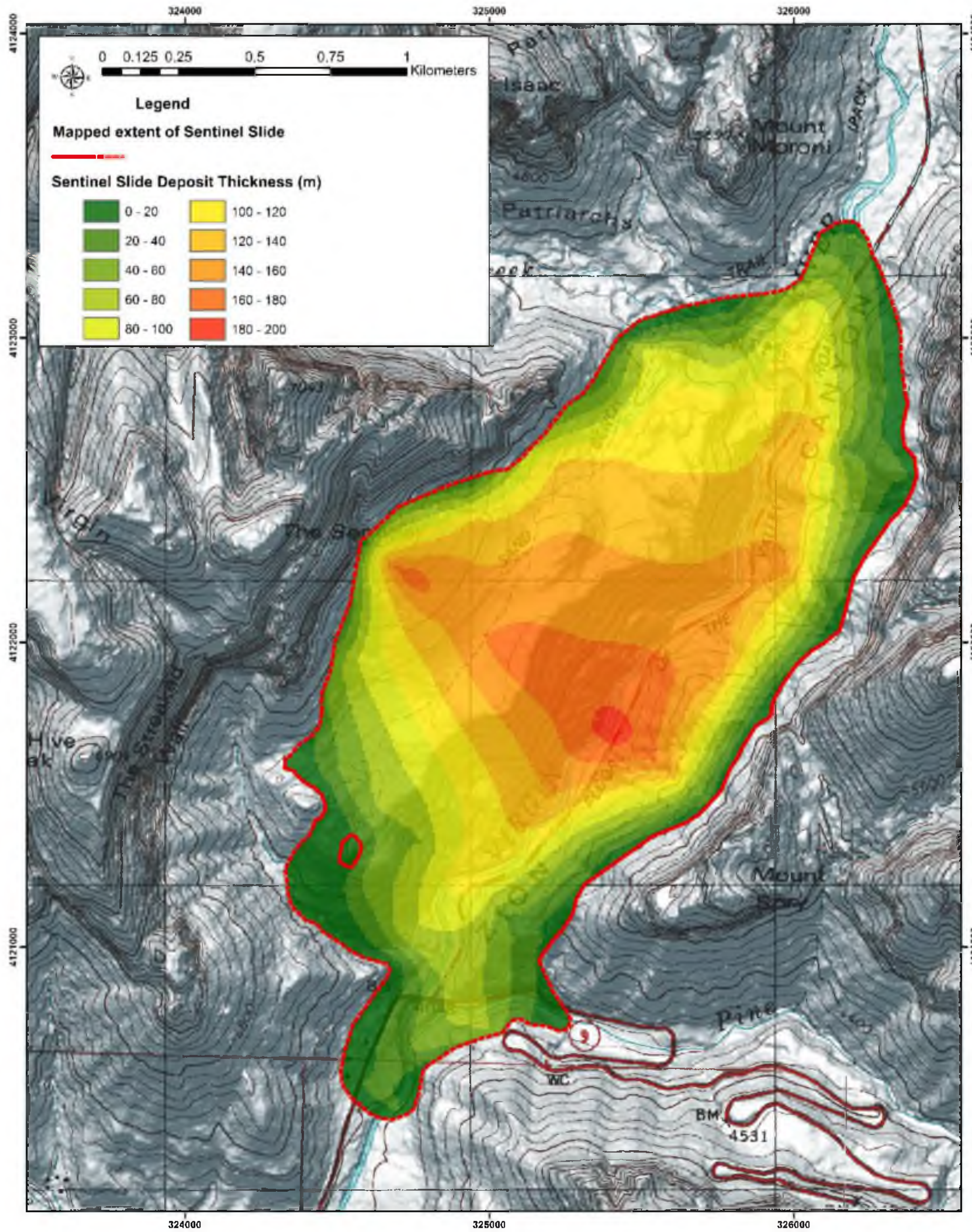


**Figure 11.** Thickness of the Sentinel rock avalanche deposit immediately after failure.

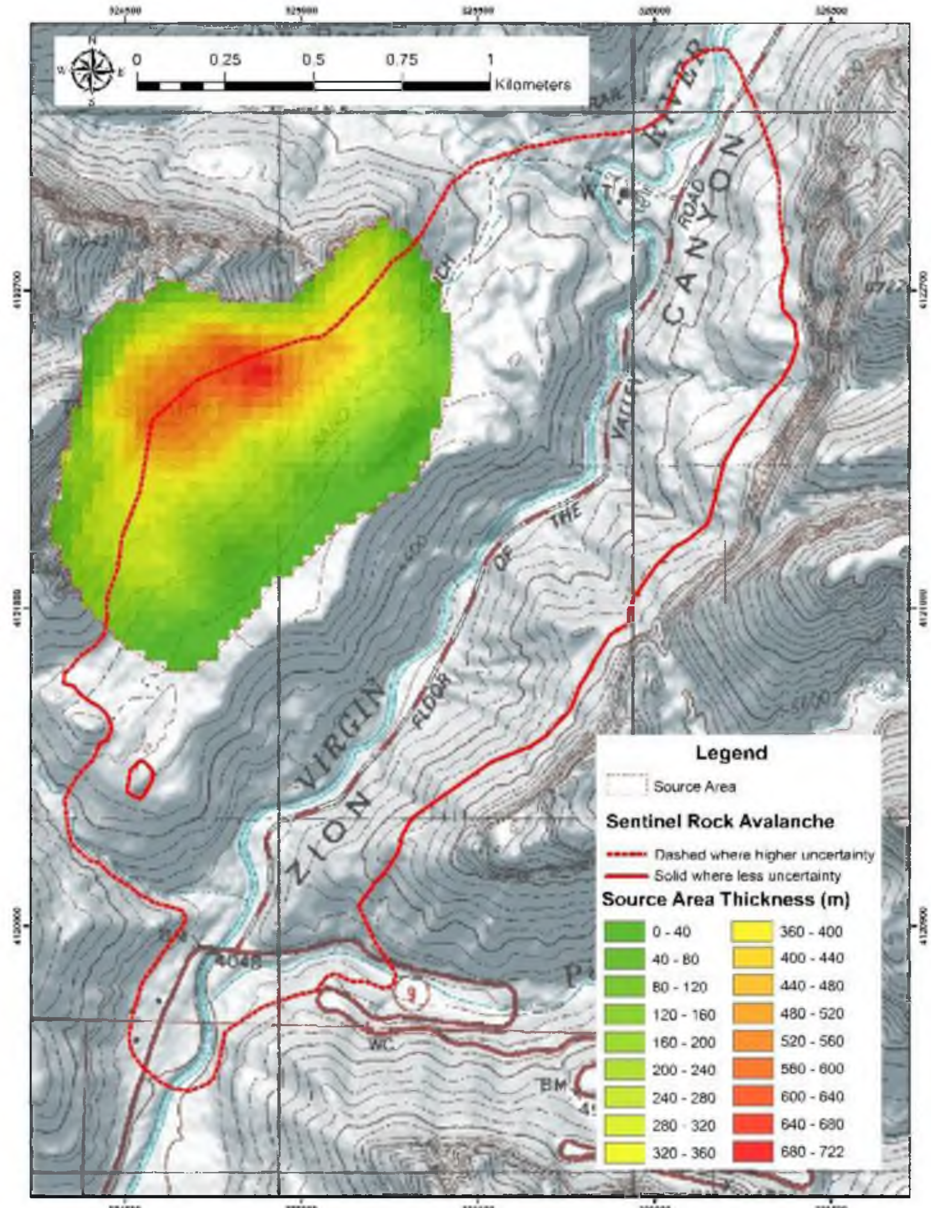


**Figure 12.** Thickness of the source area before failure.

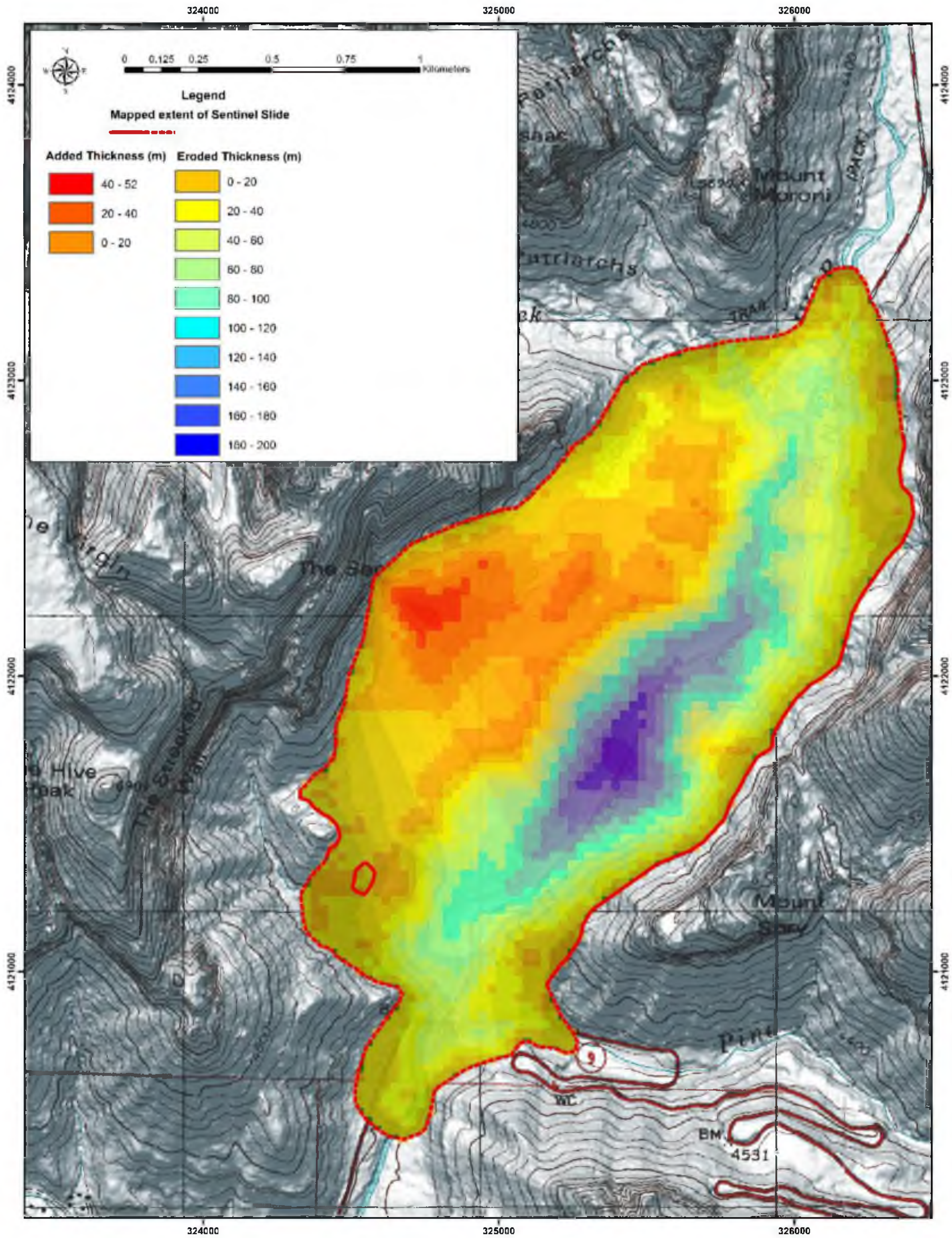


**Figure 13.** Thickness eroded by the Virgin River, also showing locations where material has been added by mass wasting from surrounding cliffs.

**Figure 14.** Photograph of large post-slide sandy talus cone, a prominent feature of the Sentinel rock avalanche deposit area.

# 4. COSMOGENIC NUCLIDE SURFACE EXPOSURE DATING

## 4.1 Dating

Cosmogenic nuclide surface exposure dating was used to determine the age of Sentinel rock avalanche deposits. Direct dating is crucial in determining the mechanisms involved in the failure, as well as rates of subsequent landscape modification. Bedrock involved in the Sentinel rock avalanche is predominantly Jurassic sandstone rich in quartz. The cosmogenic nuclide $^{10}Be$ is ideal for dating quartz-rich rock (Ivy-Ochs and Kober, 2008).

## 4.2 Sampling

Boulders for cosmogenic nuclide dating were selected during field mapping. Boulders were chosen based on dip of the surface and overall size, to maximize cosmic ray exposure. The sandstone is friable and has been eroded since deposition in the rock avalanche deposit. Boulders with little weathering and erosion which were determined to be undisturbed since deposition were preferred. To ensure complete spatial coverage of the rock avalanche deposit, twelve samples were taken: ten encompassing the north-south extent of the western portion, and two from the southeast portion (Figure 15). Complete spatial coverage should yield a more robust indication of timing, as well as to determine whether the deposit formed in one or multiple avalanches.

Samples were cut from each boulder in the field using a battery-powered rock saw, and then removed with a hammer and chisel. Location coordinates, elevation, boulder dimensions, lithology, and topographic shielding were noted for each boulder sampled. Sample logs with photographs are included in Appendix B. Figures 16 and 17 illustrate a typical boulder for sampling and sample extraction. Inherited $^{10}Be$ can occur in bedrock if the surface was exposed to cosmic rays before deposition on the landslide surface (Ivy-Ochs and Kober, 2008). Care was taken to sample surfaces that were not exposed to cosmic rays prior to deposition; highly weathered faces or surfaces with desert varnish were thus avoided. Efforts were made following sampling to remediate the remaining surfaces to natural looking forms.

4.3 Methods

Samples were crushed and sieved to obtain at least 800 g of material for transport and analysis (Figure 18). Samples were taken to the ETH Zurich AMS facility in Switzerland for preparation and $^{10}Be$ cosmogenic nuclide analysis. Pure quartz must be extracted from the sandstone to measure cosmogenic $^{10}Be$. First, the samples were subjected to selective chemical dissolution in a hot ultrasonic bath and on a shaker table. Second, diluted HF was added to the solution to dissolve minerals other than quartz. After pure quartz was obtained (Figure 19) a $^{9}Be$ carrier was added prior to completely dissolving the quartz. Concentrated HF and $HNO_3$ were then used to dissolve the quartz, after which $^{10}Be$ was separated through precipitation. The process and procedures are described in detail by Ivy-Ochs and Kober (2008).

We calculated exposure ages with the CRONUS calculator (Balco et al., 2008) using the northeast North America calibration data set (Balco et al., 2009) and a time-dependent spallation production model (Lal, 1991; Stone, 2000). Production rates were corrected to account for topographic shielding and dip of the sampled surface. Iron concretions in several boulders were weathering resistant, standing 1-2 cm above the surrounding rock surfaces and permitting minimum estimates of erosion since deposition; we assumed a constant erosion rate of 0.001 cm/year. All data used to calculate $^{10}$Be exposure ages are shown in Table 2.

4.4 Exposure Ages

Cosmogenic $^{10}$Be nuclide dating yielded a mean failure age for the Sentinel rock avalanche of 4.8 ± 0.4 ka (Figure 20). Nine of the twelve samples were used to determine this mean failure age and standard deviation, while three samples were regarded as outliers and not included in the calculation. For comparison, we also determined the age using the camel plot approach which shows a summary of probability diagrams (Balco, 2011), which yielded an exposure age for the slide of 4.74 ka (Figure 21), nearly identical to our preferred mean age. Similar exposure ages were found for boulders across the surface of the rock avalanche deposit (Figure 22), indicating simultaneous deposition in a single, massive, and catastrophic rock slope failure.

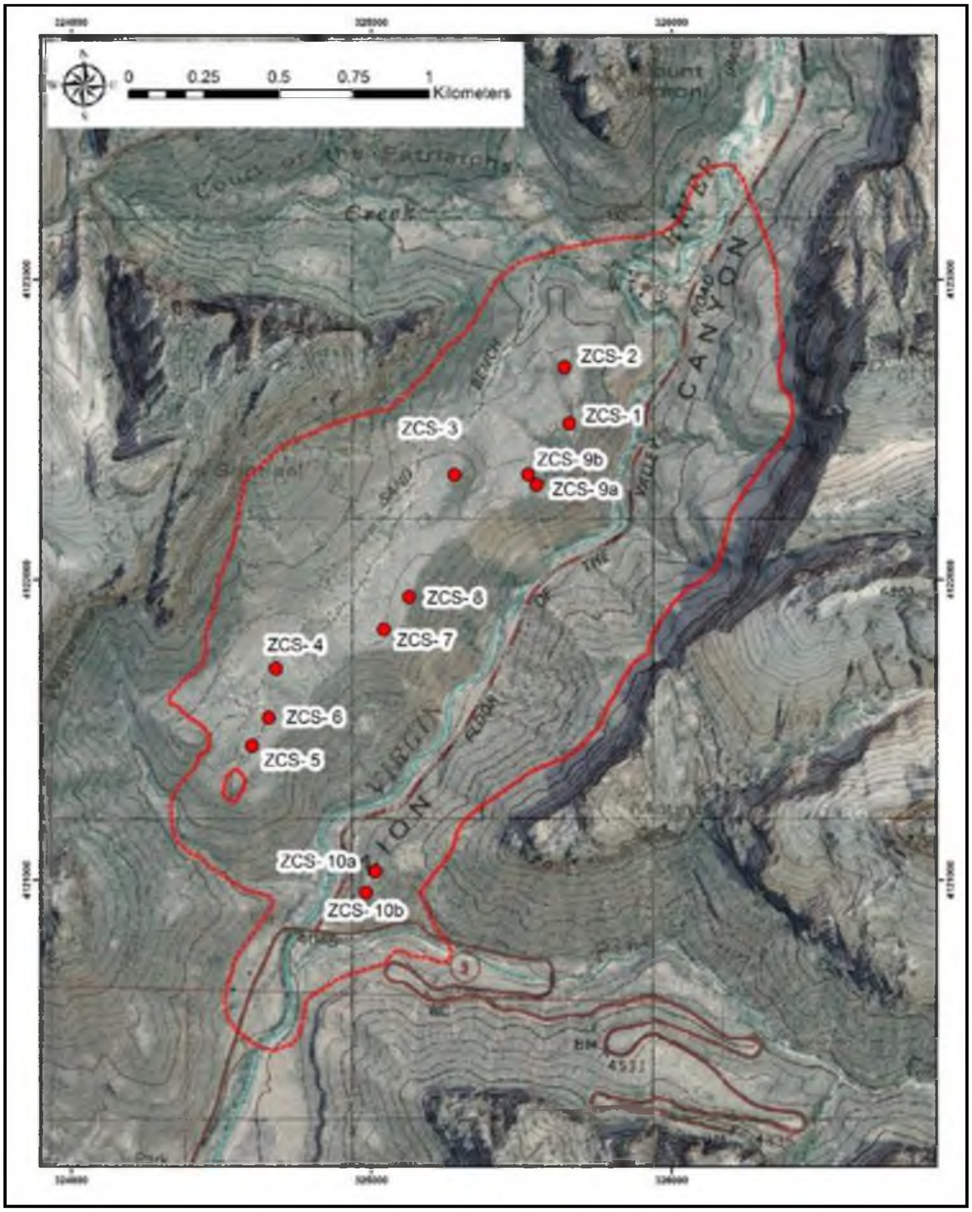


**Figure 15.** Locations of sampled boulders spanning the rock avalanche deposit.

**Figure 16.** Boulder ZCS-5.

**Figure 17.** Photograph of sample extraction (visible between the clear ruler and the tape measure). Samples extracted in the field were approximately 15 cm wide, 30 cm long, and 1.5 cm deep.


**Figure 18.** Crushed rock for transport to the ETH Zurich AMS facility.

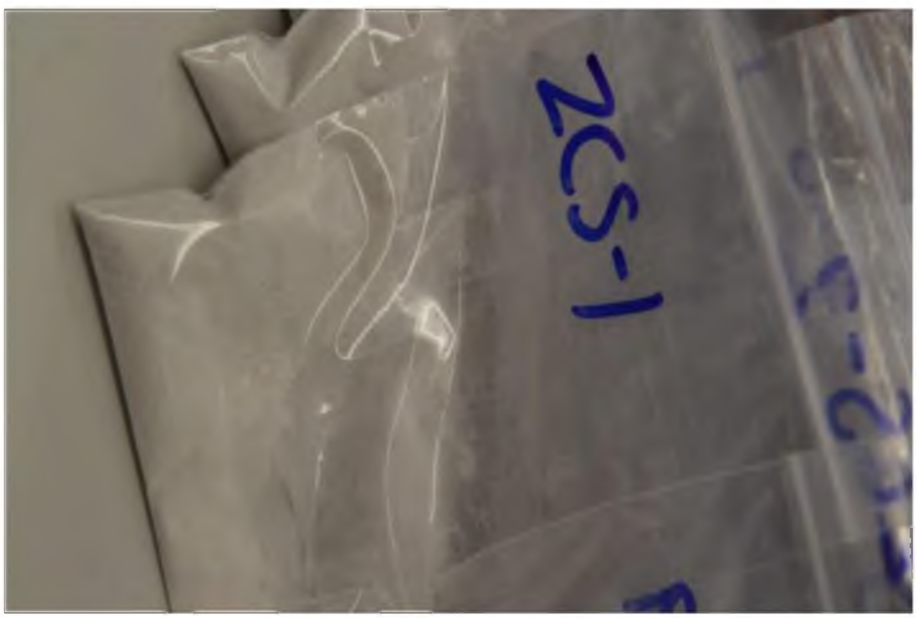


**Figure 19.** Extracted quartz.

**Table 2.** Sample locations and parameters for cosmogenic dating.

| Sample | Latitude | Longitude | Elevation | Thickness | Shielding | Erosion rate | Be-10 | +/- | Exposure age | Uncertainty |
|---|---|---|---|---|---|---|---|---|---|---|
| *name* | *(DD)* | *(DD)* | *(m)* | *correction* | *correction* | *(cm yr-1)* | *atoms g-1* | *atoms g-1* | *(yr)* | *external (yr)* |
| ZCS-1 | 37.2329 | -112.9653 | 1387 | 0.990 | 0.963 | 0.001 | 66409 | 26069 | 6619 | 2745 |
| ZCS-2 | 37.2346 | -112.9655 | 1382 | 0.990 | 0.962 | 0.001 | 50126 | 12289 | 5141 | 1333 |
| ZCS-3 | 37.2313 | -112.9696 | 1438 | 0.988 | 0.951 | 0.001 | 43369 | 11550 | 4378 | 1223 |
| ZCS-4 | 37.2254 | -112.9761 | 1398 | 0.986 | 0.934 | 0.001 | 80512 | 16405 | 8266 | 1837 |
| ZCS-5 | 37.2230 | -112.9770 | 1387 | 0.990 | 0.947 | 0.001 | 40201 | 8457 | 4229 | 941 |
| ZCS-6 | 37.2239 | -112.9764 | 1389 | 0.986 | 0.946 | 0.001 | 46174 | 8454 | 4828 | 947 |
| ZCS-7 | 37.2266 | -112.9721 | 1435 | 0.988 | 0.964 | 0.001 | 47223 | 7683 | 4693 | 824 |
| ZCS-8 | 37.2276 | -112.9712 | 1440 | 0.990 | 0.966 | 0.001 | 68384 | 9940 | 6546 | 1051 |
| ZCS-9a | 37.2311 | -112.9665 | 1400 | 0.990 | 0.967 | 0.001 | 45759 | 8459 | 4639 | 916 |
| ZCS-9b | 37.2314 | -112.9668 | 1403 | 0.990 | 0.968 | 0.001 | 46333 | 9873 | 4683 | 1058 |
| ZCS-10a | 37.2193 | -112.9722 | 1291 | 0.986 | 0.967 | 0.001 | 52935 | 10341 | 5729 | 1201 |
| ZCS-10b | 37.2187 | -112.9726 | 1283 | 0.986 | 0.970 | 0.001 | 42800 | 9173 | 4720 | 1073 |

CRONUS-Earth 10Be exposure age calculator

Balco et al., 2009: Northeast North America calibration

Time-dependent production, Lal (1991)/Stone (2000)

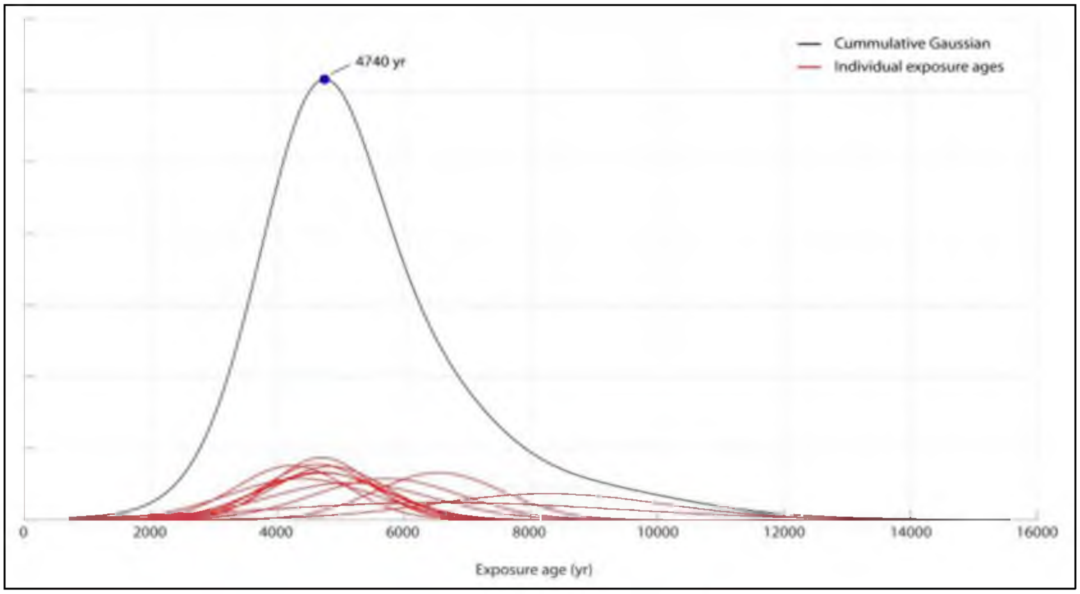


**Figure 20.** Camel plot of $^{10}$Be ages highlighting the mean exposure age.

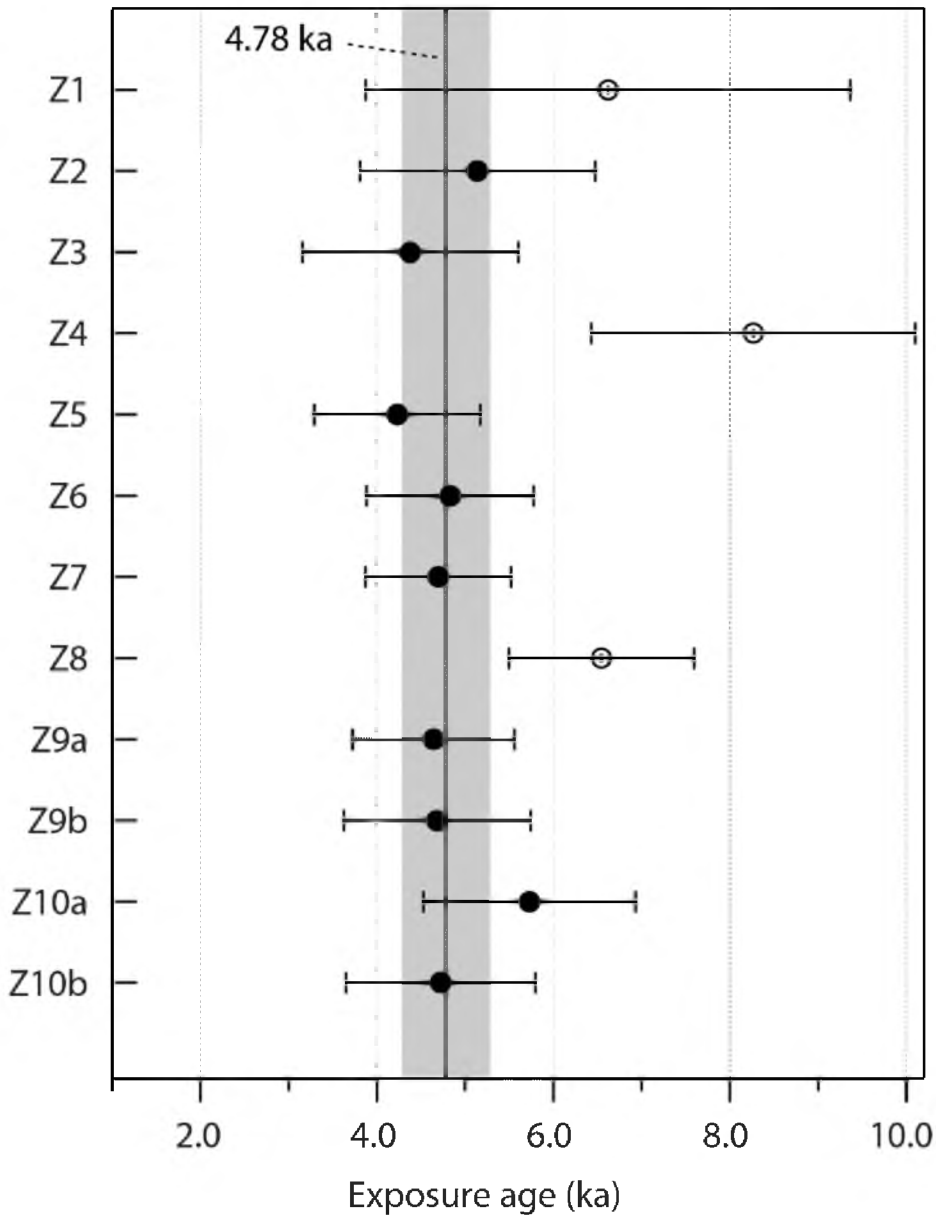


**Figure 21.** $^{10}Be$ exposure age for each sample with error. Open circles are outliers not included in determining the mean age shown.

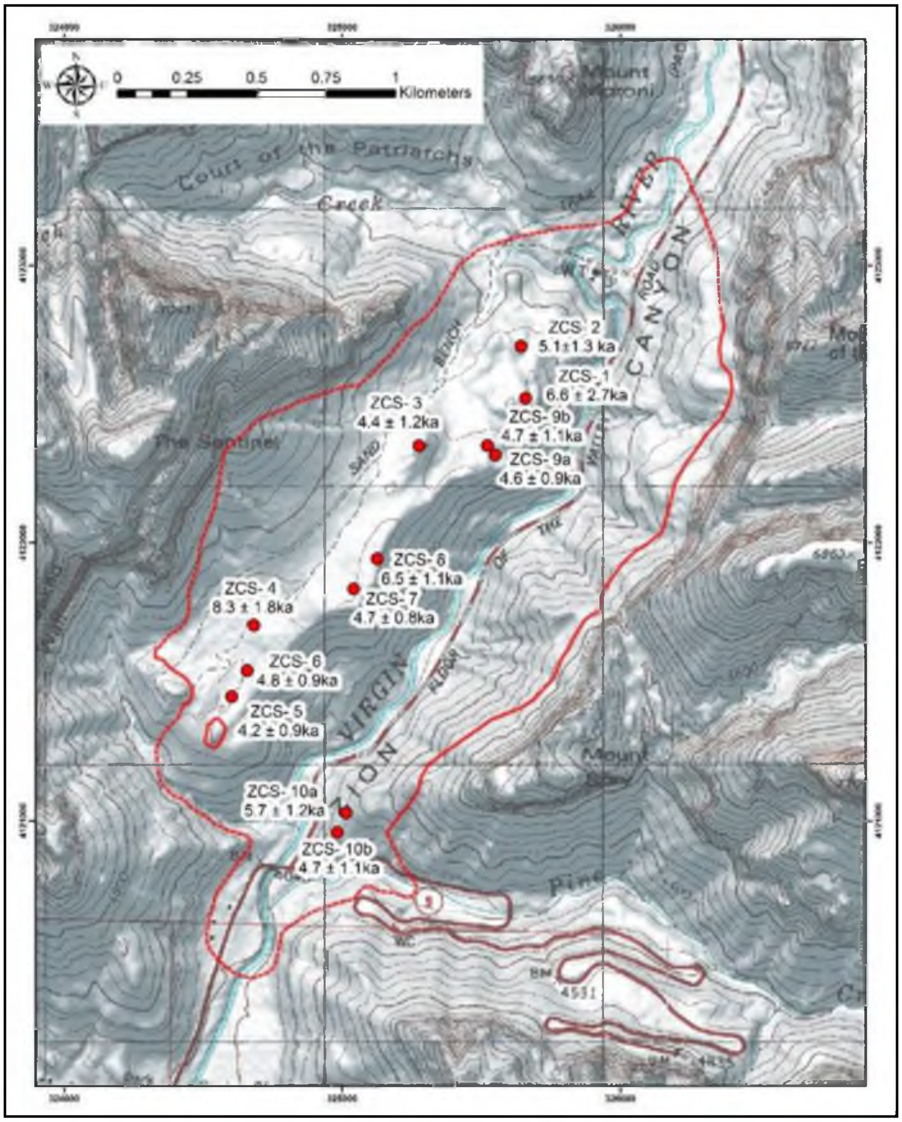


**Figure 22.** Sample locations with $^{10}$Be exposure age for each.

# 5. RUNOUT MODELING

## 5.1 Methods

Rock avalanches are complex dynamic phenomena and challenging to model given inherent uncertainties in pre-failure topographic reconstruction. We implemented a simplified dynamic analysis using DAN3D, which simulates rock avalanche runout over arbitrary 3D terrain (McDougall and Hungr, 2006). Developed to simulate rapid flow slides, debris flows, and rock avalanches (Davies and McSaveney, 2002), DAN3D is an "equivalent-fluid" code that treats the mass movement as a frictional fluid and allows user selection of basal rheology and shear resistance parameters (Hunger, 1995; Mcdougall and Hungr, 2004; Sosio et al., 2008; Pirulli, 2009; Nagelisen et al., 2015). Rheology is selected on the basis of back analysis of the landslide parameters including the total horizontal runout distance, the length of the deposit, and the mean thickness of the deposit (Hungr and Evans, 1996). The Voellmy rheology is a two-parameter model containing a friction coefficient and a turbulence term, the latter dependent on the square of the flow velocity and the density of debris (Hungr and Evans, 1996), and is commonly used to simulated rock avalanche runout. DAN3D also requires input of flow-path geometry, thickness of the source, density, and rates of deposition or entrainment of basal material (here neglected) (Davies and McSaveney, 2002).

5.2 Runout Analysis Results

Empirical evaluation of the Fahrböschung, or travel angle, is often used in back analysis of rock avalanche dynamics. Fahrböschung is the angle between a horizontal plane and a line connecting the top of the source area to the most distal toe portion of the deposit (Stock and Uhrhammer, 2010). Lower Fahrböschung values indicate higher mobility (McDougall et al., 2012). The calculated Fahrböschung of 18–20° for the Sentinel slide suggests relatively low mobility for its volume compared to other global case histories (Figure 23).

The results of DAN3D analysis are shown in Figure 24a-d. The Voellmy friction parameter was set to 0.27 and turbulence parameter to 200. The internal friction angle was held constant at 35°, and the unit weight was 20 kN/m. Only one basal material unit was used, i.e., parameters were constant in space. Modelling suggests a very rapid, catastrophic rock avalanche. The simulation was run for 200 s, but most of the movement was complete by 60 s, and the valley was crossed within only 20 s with a maximum velocity of 90 m/s. The material ran up the cliffs on the eastern side of the valley after rapidly crossing the path of the Virgin River, and then spread upstream and downstream where it also flowed into Pine Creek.

The modeled deposit boundaries match closely with mapped boundaries (Figure 24). Exceptions occur in the Pine Creek drainage where the modeled deposit extended farther upstream than noted in the field, in the drainage at the southwest end of the rock avalanche, and on the eastern cliff wall where modeled run up is greater than mapped.

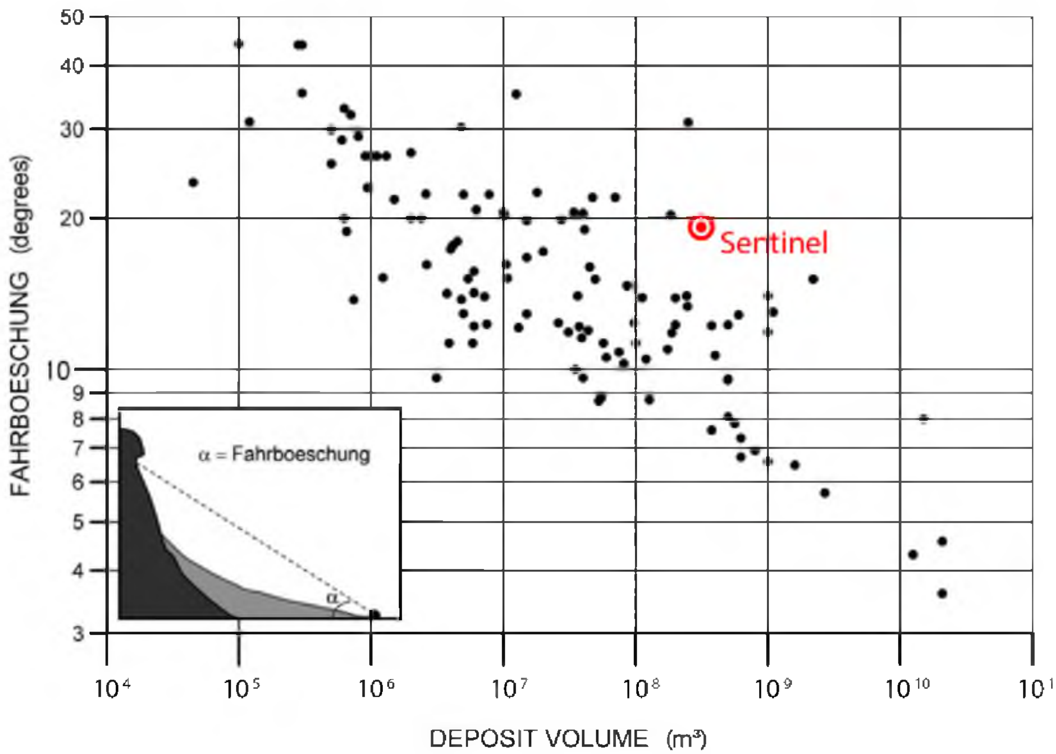


**Figure 23.** Fahrboeschung of 18-20° for the Sentinel rock avalanche suggests relatively low mobility for its volume compared to other global cases. Figure modified from Bourrier et al. (2013).

**Figure 24.** Results of DAN3D runout analysis. a) Results of runout analysis using DAN3D showing thickness and movement 5 seconds after initiation. b) Results of runout analysis using DAN3D showing thickness and movement 20 seconds after initiation. c) Results of runout analysis using DAN3D showing thickness and movement 60 seconds after initiation, most of the movement is complete by this time. d) Results of runout analysis using DAN3D showing thickness and movement of the final deposition 200 seconds after failure.

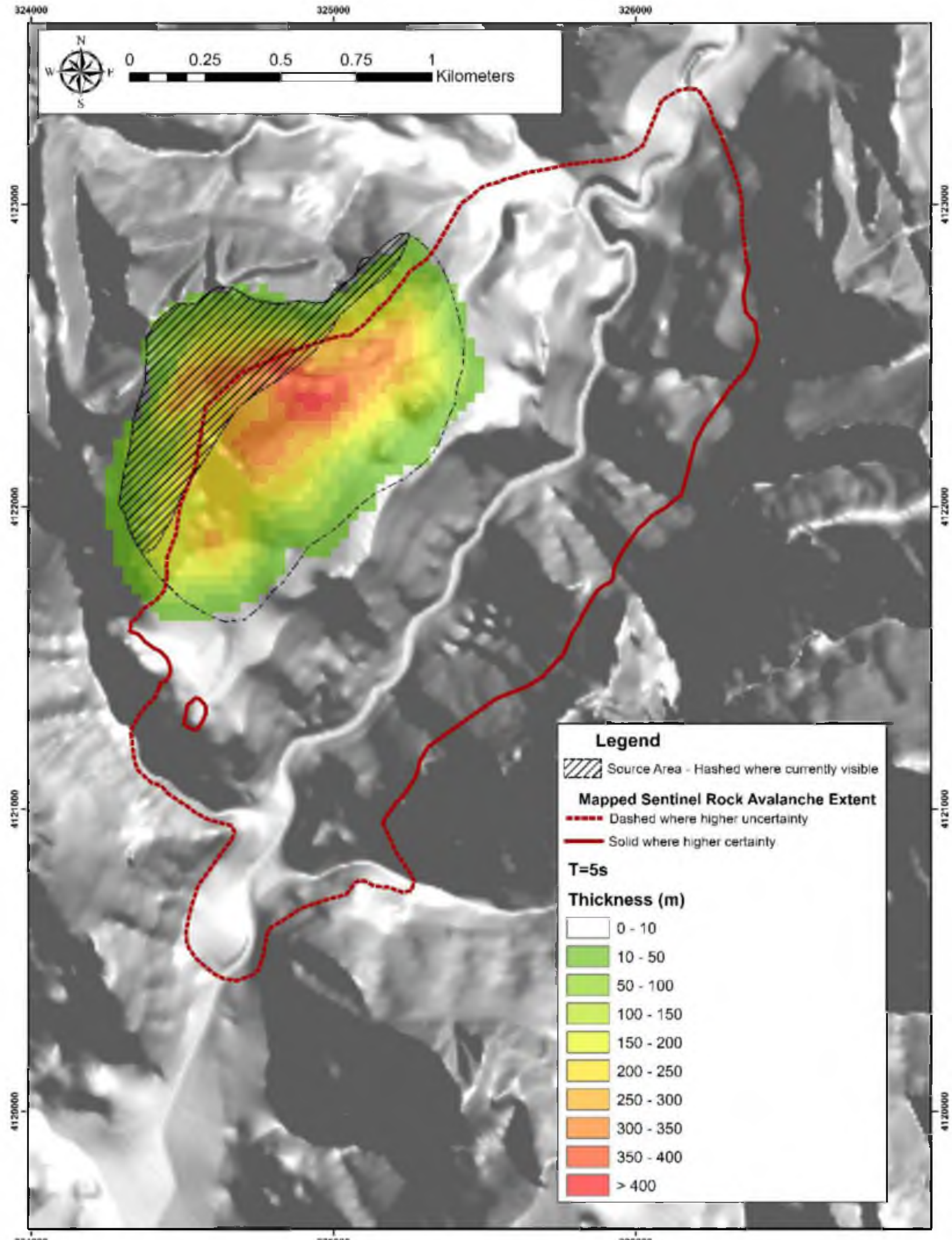


**a.**

**Figure 24.** Continued

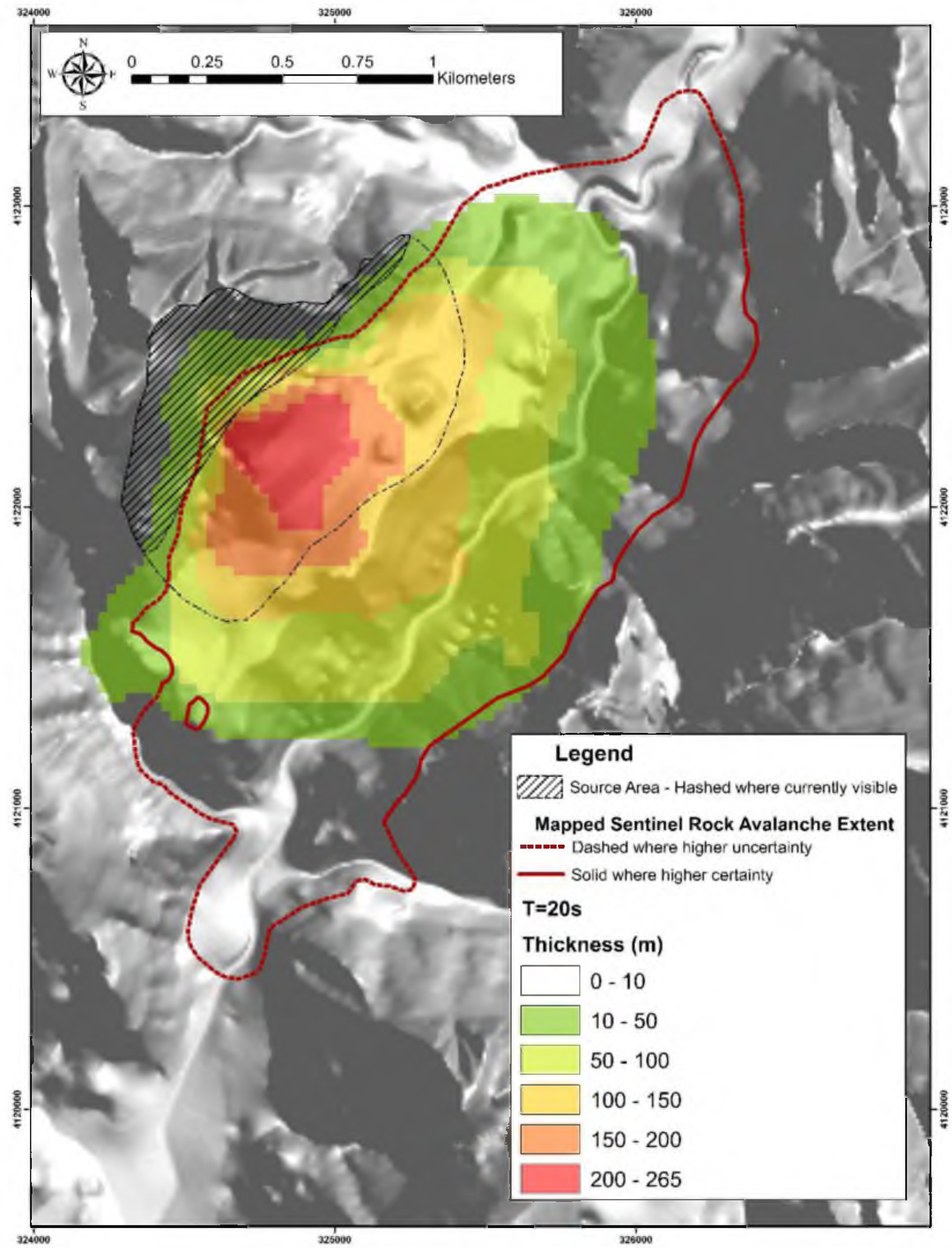


**b.**

**Figure 24.** Continued

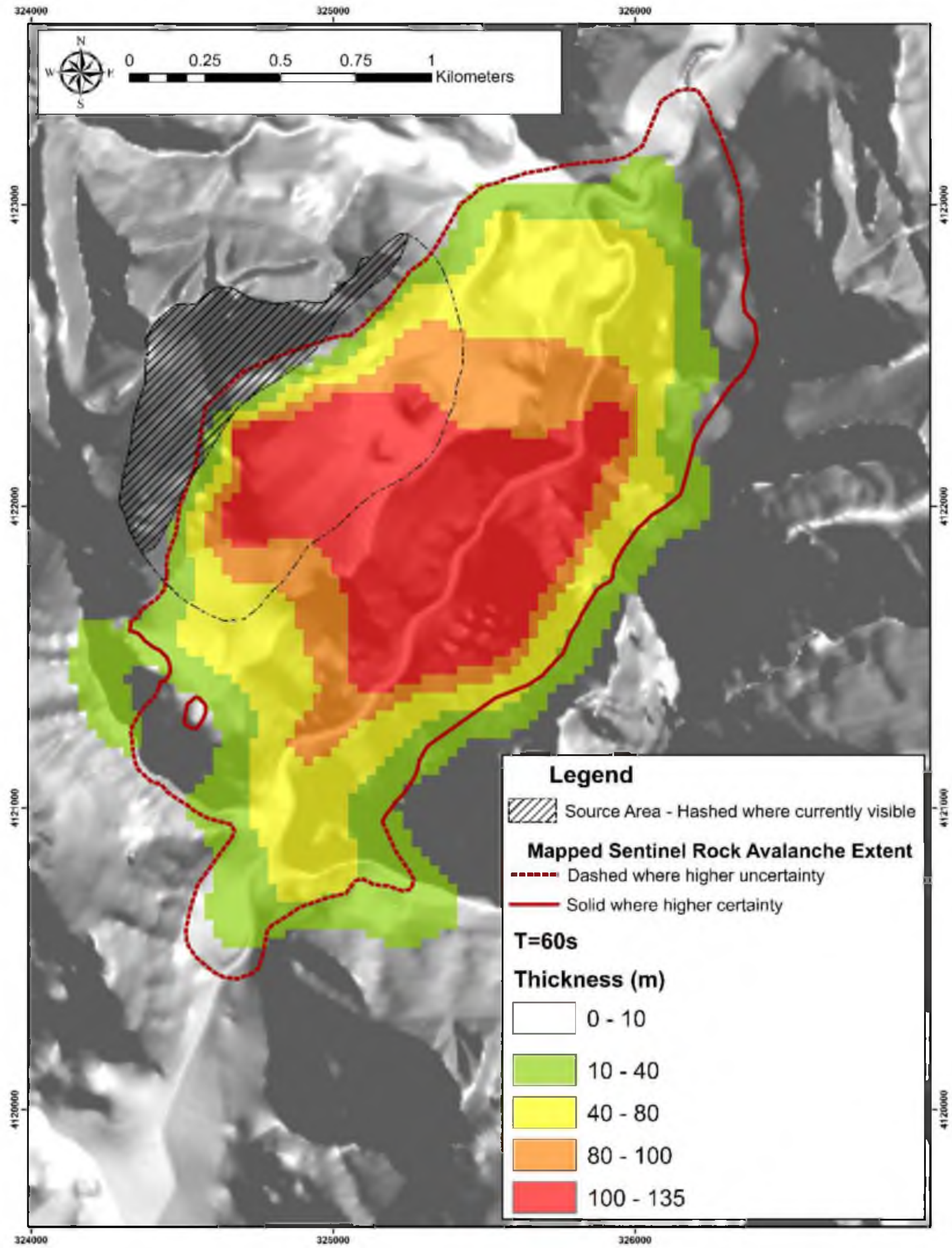


**c**.

**Figure 24.** Continued

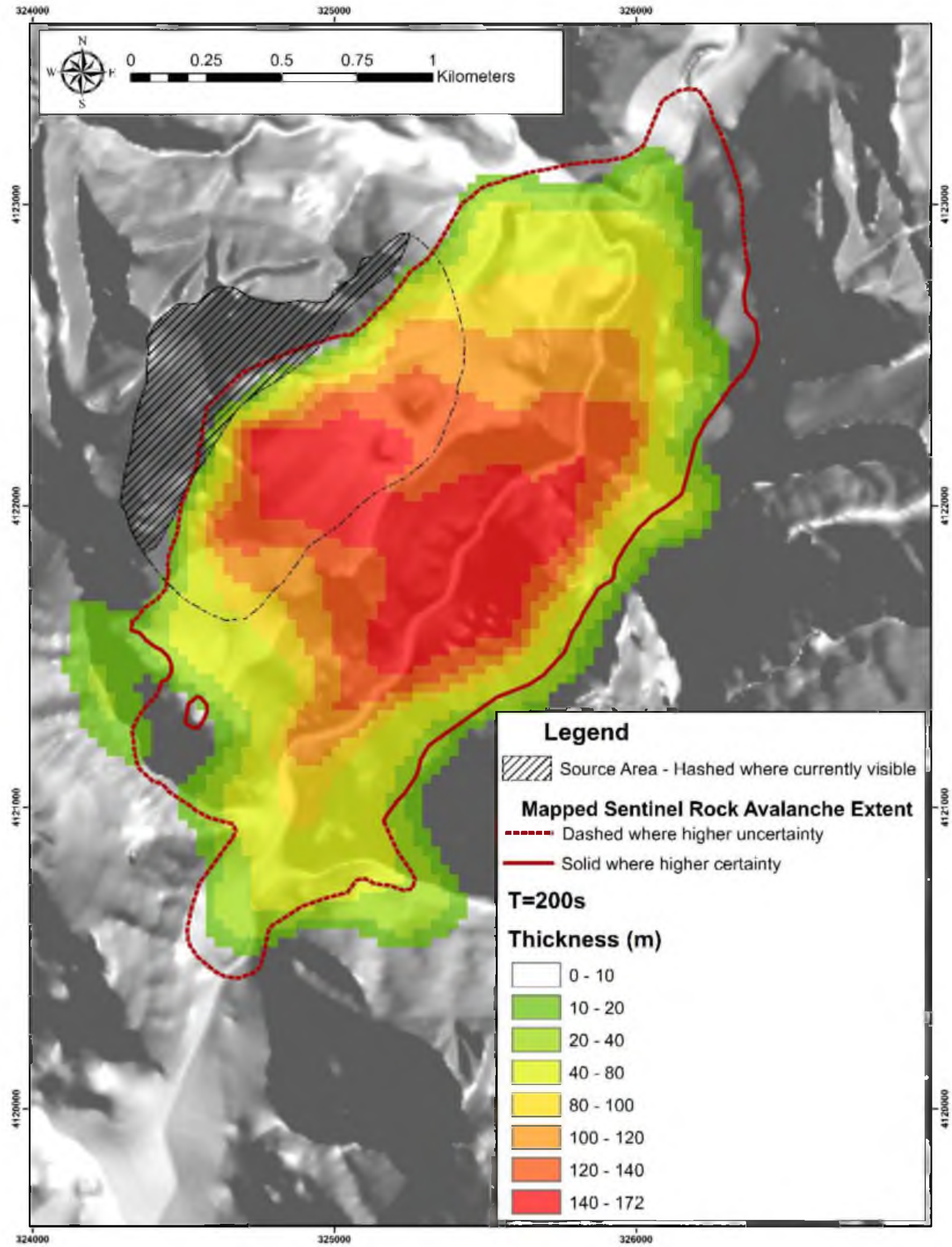


**d.**

**Figure 24.** Continued

# 6. INTERPRETATION AND DISCUSSION

## 6.1 Volume Analysis and Runout Modeling

Pre- and post-failure topographic reconstruction of the source and deposit were used to determine the area, thickness, and the volume of the rock avalanche. The deposit volume of the Sentinel rock avalanche was calculated to be 284 million $m^3$, which we deem accurate to within ± 10%. This value includes a bulking factor of about 28% as the intact rock in the source was converted to loose debris; the corresponding source volume was 227 million $m^3$. A bulking factor of 28% is well within the expected range of values for typical rock avalanches and rock slides (Hunger and Evans, 2004). The area of the slide deposit was determined to be approximately 3 million $m^2$ with an average thickness of 93 m. The eroded volume since original deposition was calculated to be 131 million $m^3$, which with a failure age of 4.8 ka equates to a deposit erosion rate of approximately 9 mm/yr. The results of the DAN3D runout modeling are consistent with the Sentinel landslide having formed as a very rapid, catastrophic rock avalanche. Mapped boundaries incorporating field observations and DEM analysis match closely with modeled deposit boundaries. This indicates that our pre-failure topography reconstruction for the base of the slide and the source area are plausible. Velocities reaching 90 m/s are within the range of expected and back-calculated values for rock avalanches (Crosta et al., 2007).

Our runout model predicts runup on the opposing eastern wall of Zion Canyon, evidence of which is not preserved today, but potentially erased by subsequent erosion.

## 6.2 Failure Timing

Cosmogenic $^{10}Be$ surface exposure dating yielded a failure age of 4.8 ± 0.4 ka. Similar exposure ages from boulders across the slide indicate simultaneous deposition and a single-event rock slope failure. Two previous radiocarbon dates obtained from charcoal in lacustrine sediment by the Utah Geological Survey (UGS) gave ages of 8009 ± 844 and 7651 ± 570 calendar years B.P. (UGS personal communication). These led to the past assumption that Sentinel Lake occupied the valley by ~8000 years B.P. These dates are, however, older than the age of the rock avalanche determined in this work. Radiocarbon dating is an indirect method for dating a landslide. The charcoal obtained from lake deposits sampled may have been older than the lake deposits.

Other past radiocarbon $^{14}C$ dating of charcoal collected in alluvial deposits yielded an age of 3930 ± 525 cal. yr B.P. (Hamilton, 1976; 1984), representing post-lake sand deposition on the clay surface. Meanwhile, a recent OSL sample from sand within lake deposits gave an age of 4.31 ± 1.3 ka B.P. (Hamilton, 2014). Together with the UGS dates, the previous interpretation was that Sentinel Lake occupied Zion Canyon for ~4000 years between ~8 – 4 ka. However, Hamilton's (2014) OSL and $^{14}C$ dates, in conjunction with our cosmogenic $^{10}Be$ age of 4.8 ka, indicate that Sentinel Lake more likely occupied Zion Canyon for approximately 600 - 800 years from 4.8 ka to ~4.1 ka. Using sediment yield calculations from the Virgin River at La Verkin, Hamilton (1976) calculated that Sentinel Lake sediments were likely deposited in a 730 year interval, consistent with our inferred date range.

## 6.3 Triggering and Failure Mechanisms

Multiple factors contributed to triggering the Sentinel rock avalanche. A key preparatory factor was likely related to development of a NNW trending slot canyon (Rogers and Engelder, 2004) near Court Of The Patriarchs (Figure 7) by erosion along a persistent discontinuity in the Navajo Sandstone. The formation of this slot canyon progressively weakened the Navajo cliff face supported by underlying Kayenta. Rapid erosion as the Virgin River undercut the Kayenta Formation at the Kayenta/Springdale contact likely then contributed to the ultimate failure.

Interpretation of geologic cross sections suggests rotational and translational movement for the initial rock slope failure. Deformed, large blocks of Navajo and Kayenta observed within the rock avalanche deposit at near stratigraphically correct elevations indicate translational movement across the relatively flat pre-failure valley floor. The cross-valley failure orientation contributed to high runup on the eastern wall, as well as the spreading of material up and downstream as it filled Zion Canyon.

Strong ground shaking in Zion National Park is possible due to the proximity of active faults. A strong earthquake could have contributed to failure of the Sentinel rock avalanche, but further investigation of paleoseismic events must be examined for the age range of interest. Pollen evidence suggests a climate similar to today (Hamilton, 2014) with warm and cold extremes. Large flash floods are common and can move significant amounts of material and debris when they occur. Flash floods could contribute to rapid undercutting of the Kayenta contributing to failure. Future research investigating paleoseismicity and paleoclimate is warranted.

# 7. CONCLUSION

The Sentinel rock avalanche was a large landslide that transformed the late Holocene geomorphology of Zion Canyon. Reconstructing topography before and after the event, we estimate that the volume of the Sentinel rock avalanche was 284 million $m^3$; the deposit area is approximately 3 million $m^2$ with an average thickness of 93 m. The rock avalanche created a dam in Zion Canyon 3.3 km in length blocking the Virgin River and Pine Creek. Thick lacustrine and alluvial sediments currently exposed in Zion Canyon are evidence of Sentinel Lake which formed behind this debris. The Virgin River is aggressively cutting into the landslide deposit since breaching the blockage, and has removed ~131 million $m^3$ of material or 45% of the original deposit volume. The calculated deposit erosion rate based on a failure age of 4.8 ka is approximately 9 mm/yr.

Results of 3D numerical runout modeling are consistent with catastrophic failure of the Sentinel rock avalanche, i.e., rapidly and suddenly and as a single event. The rock avalanche crossed the valley in ~20 s, rapidly obstructing the path of the Virgin River, and ran up the cliffs on the eastern side of the valley. After crossing the valley, material spread upstream and downstream where it also flowed into Pine Creek, likely damming it as well. Most of the movement was complete within ~60 s. Maximum estimated velocity was 90 m/s. The mapped slide extent matches well with the modeled deposit boundaries, indicating that our pre-failure topography reconstruction and volume analysis are plausible.

Cosmogenic $^{10}$Be surface exposure dating yielded a failure age of 4.8 ± 0.4 ka. Similar ages were found for boulders from across the surface of the slide are consistent with the hypothesized single-event catastrophic failure scenario. Interpretation of radiocarbon dating results from past investigations, and an OSL sample from lake deposits, indicate that Sentinel Lake filled with sediment ~4000 years ago. Sentinel Lake thus likely occupied Zion Canyon for approximately 600-800 years.

The Sentinel rock avalanche was initiated by multiple factors. Erosion of a slot canyon near court of patriarchs likely weakened the Navajo cliff supported by underlying Kayenta, while rapid erosion into the Kayenta and at the Kayenta/Springdale contact by the Virgin River undermined the already burdened material. Future research should investigate climatic factors involved and the possibility of a seismic trigger. Rock fall and landslide hazards present an ongoing threat in the dynamic desert environments of the American southwest. This work demonstrates the susceptibility of massive sandstone units to rock avalanche hazards. The behavior modeled shows that fast moving, catastrophic landslides can occur in areas with similar topography and erosional factors. This may be used as a foundation for hazard assessment in similar landscapes.

# APPENDIX A

# CROSS SECTIONS

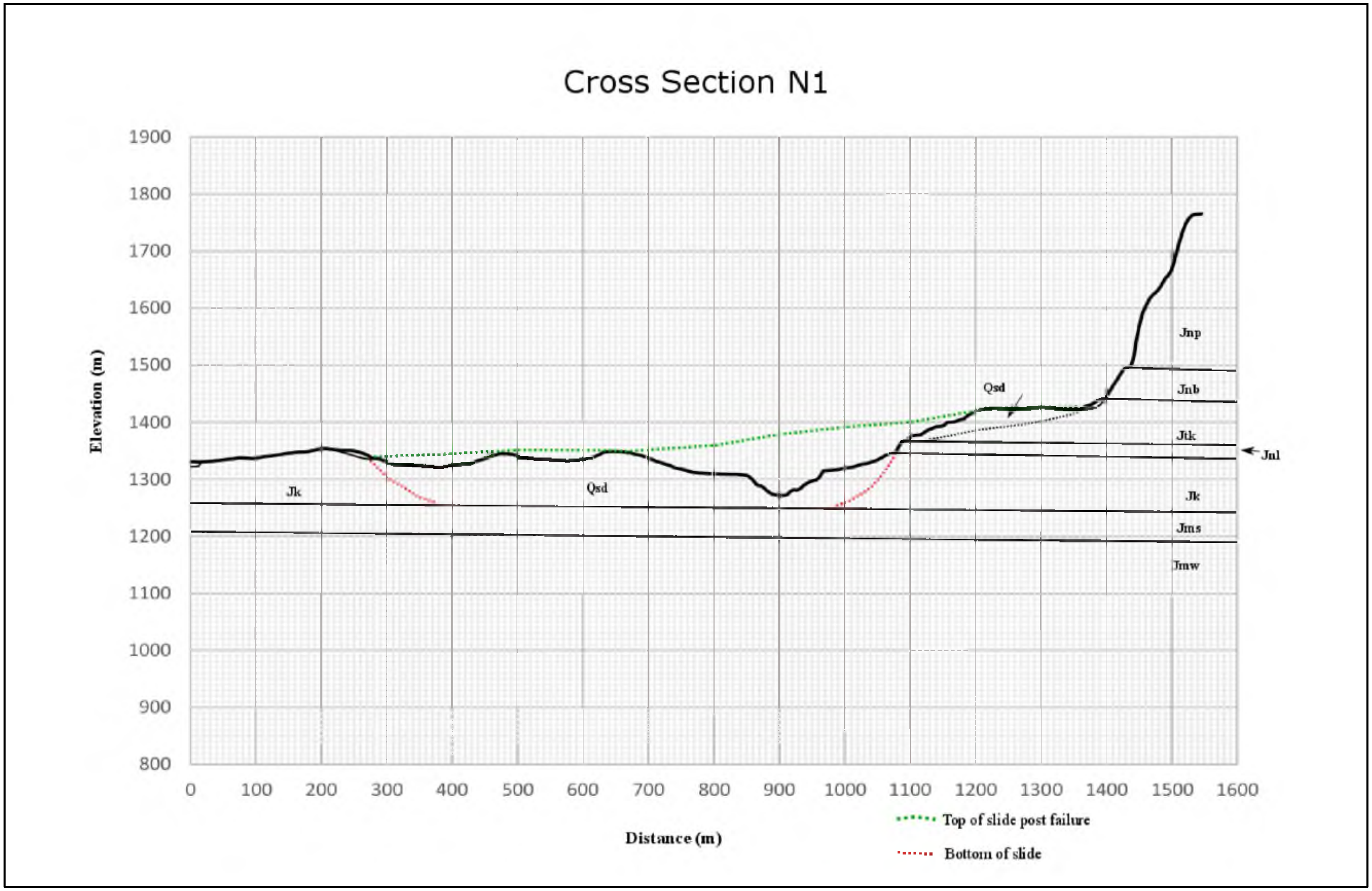


**Figure 25**. Cross section N1.

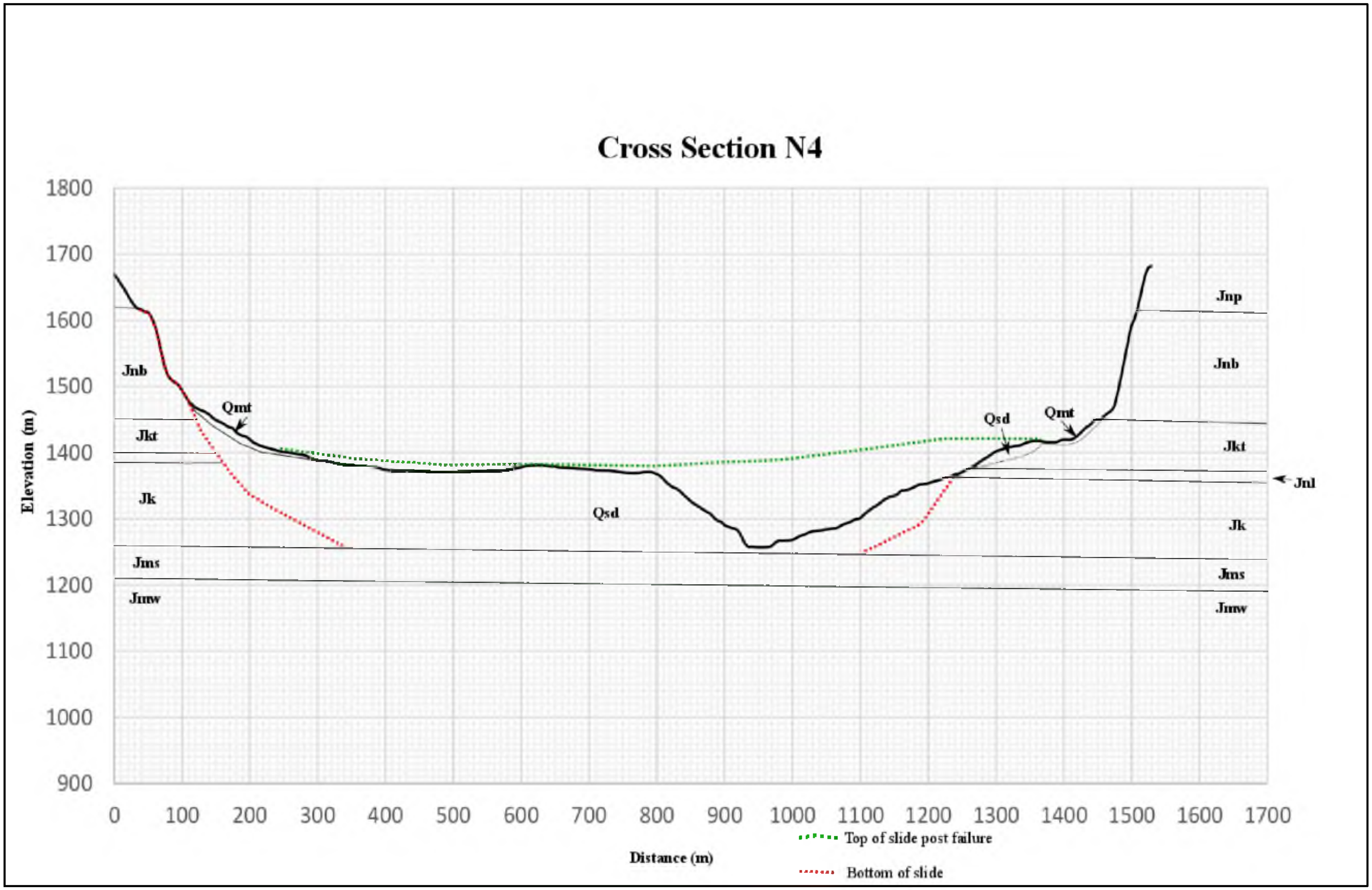


**Figure 26.** Cross section N4.

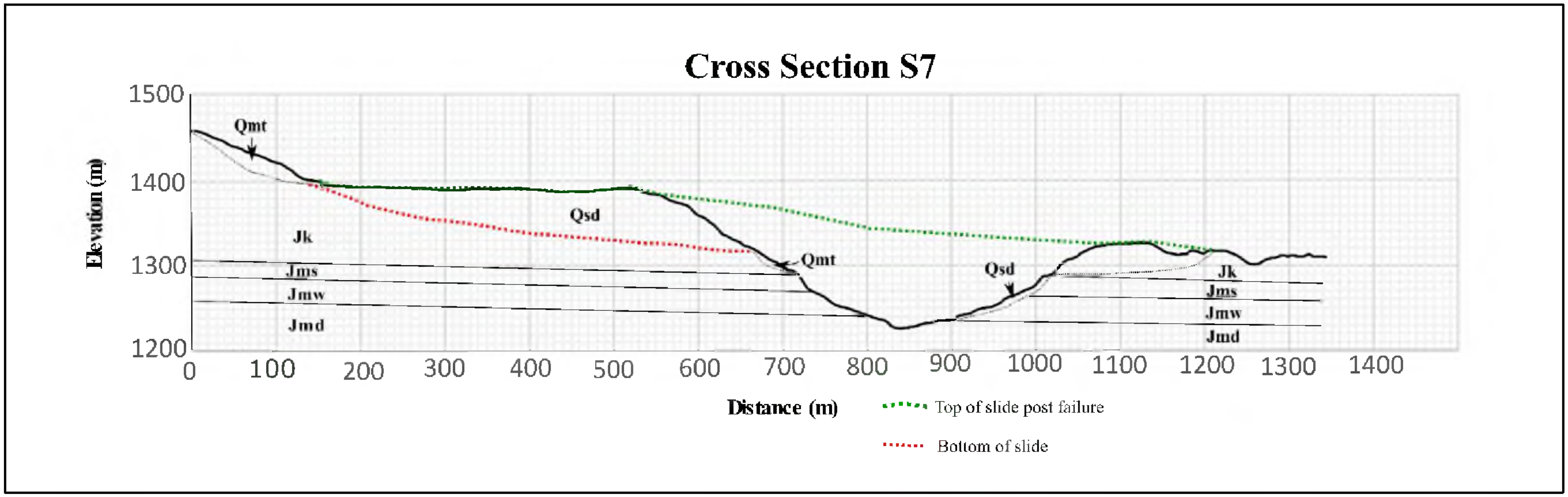


**Figure 27.** Cross section S7.

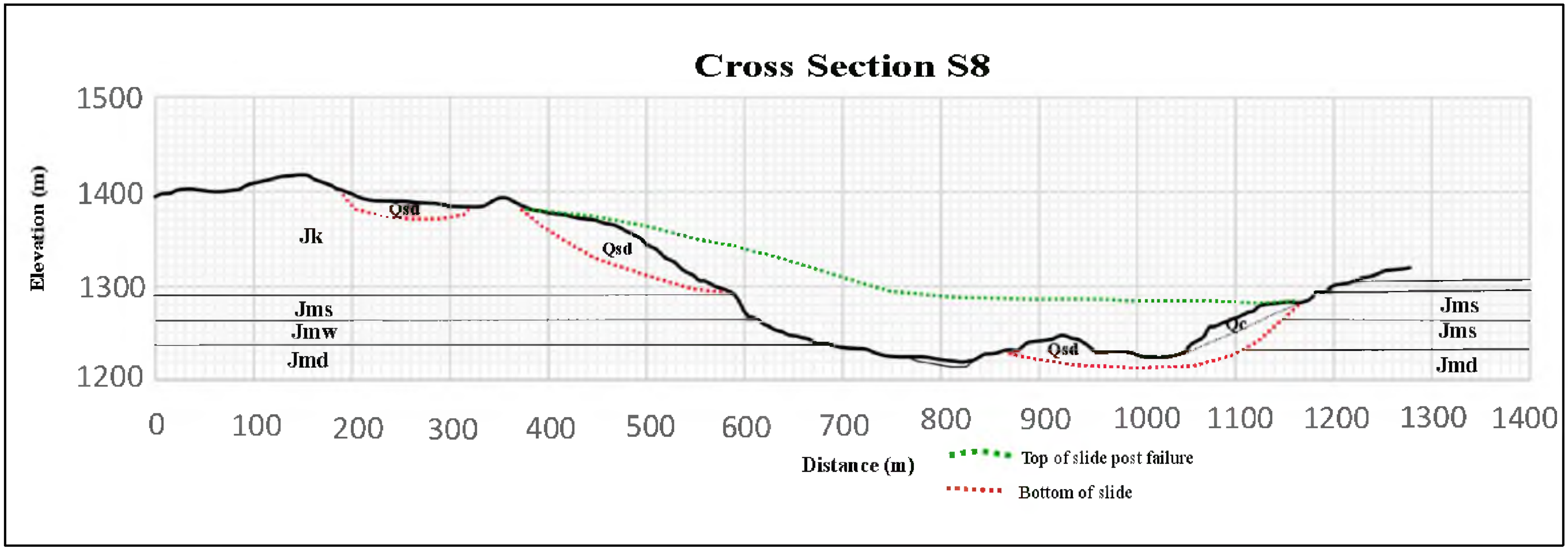


**Figure 28.** Cross section S8.

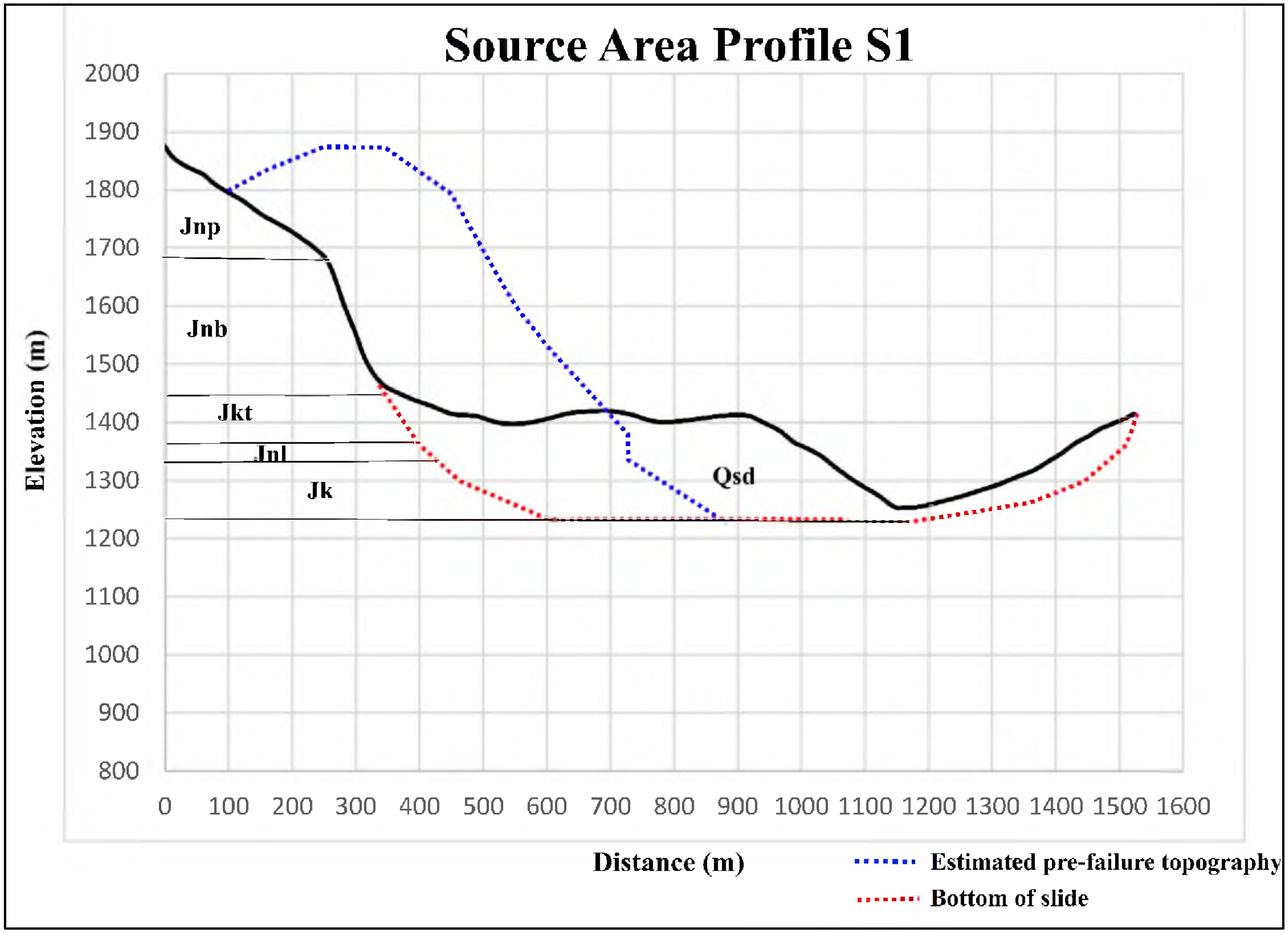


**Figure 29.** Cross section S1.

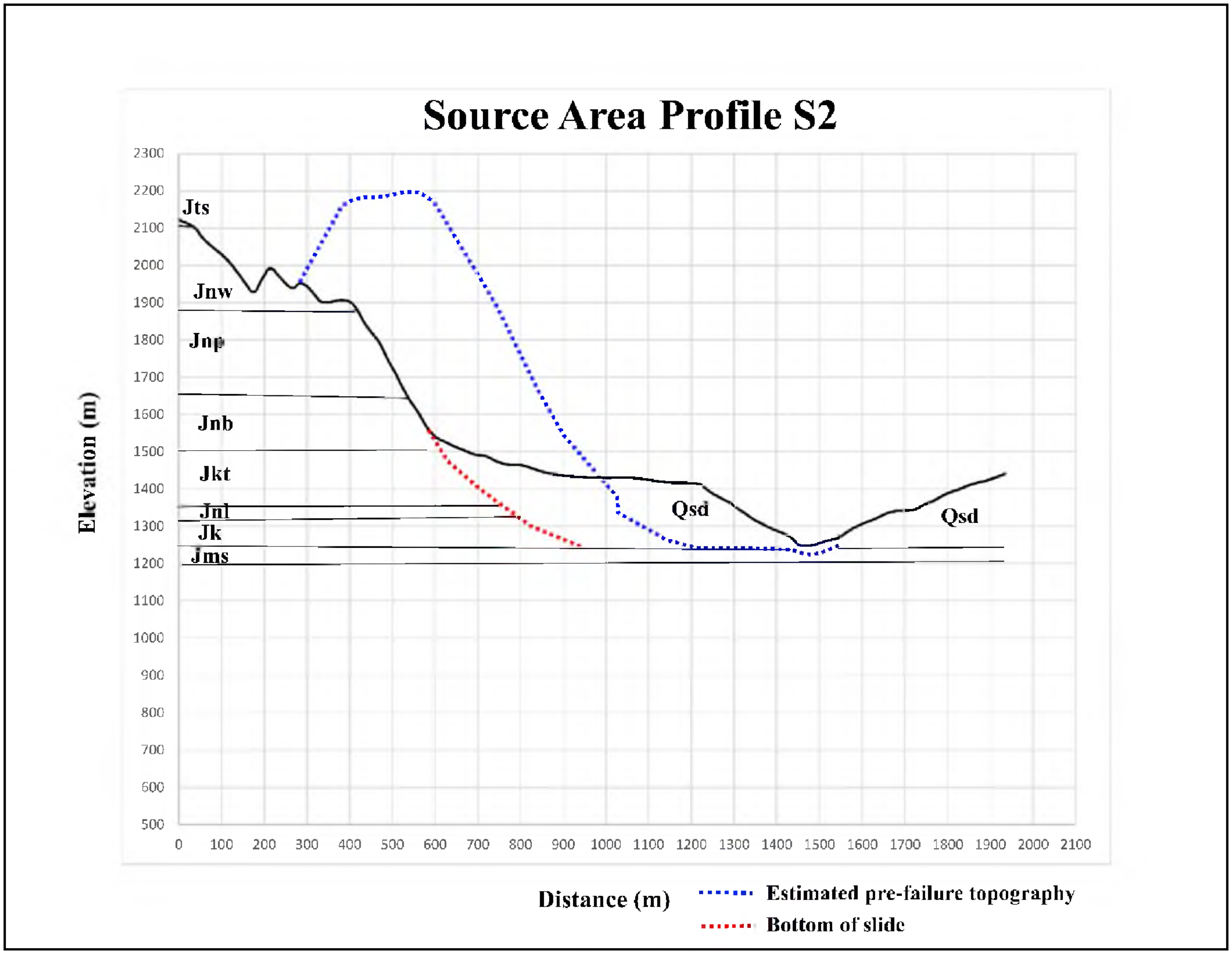


**Figure 30.** Cross section S2.

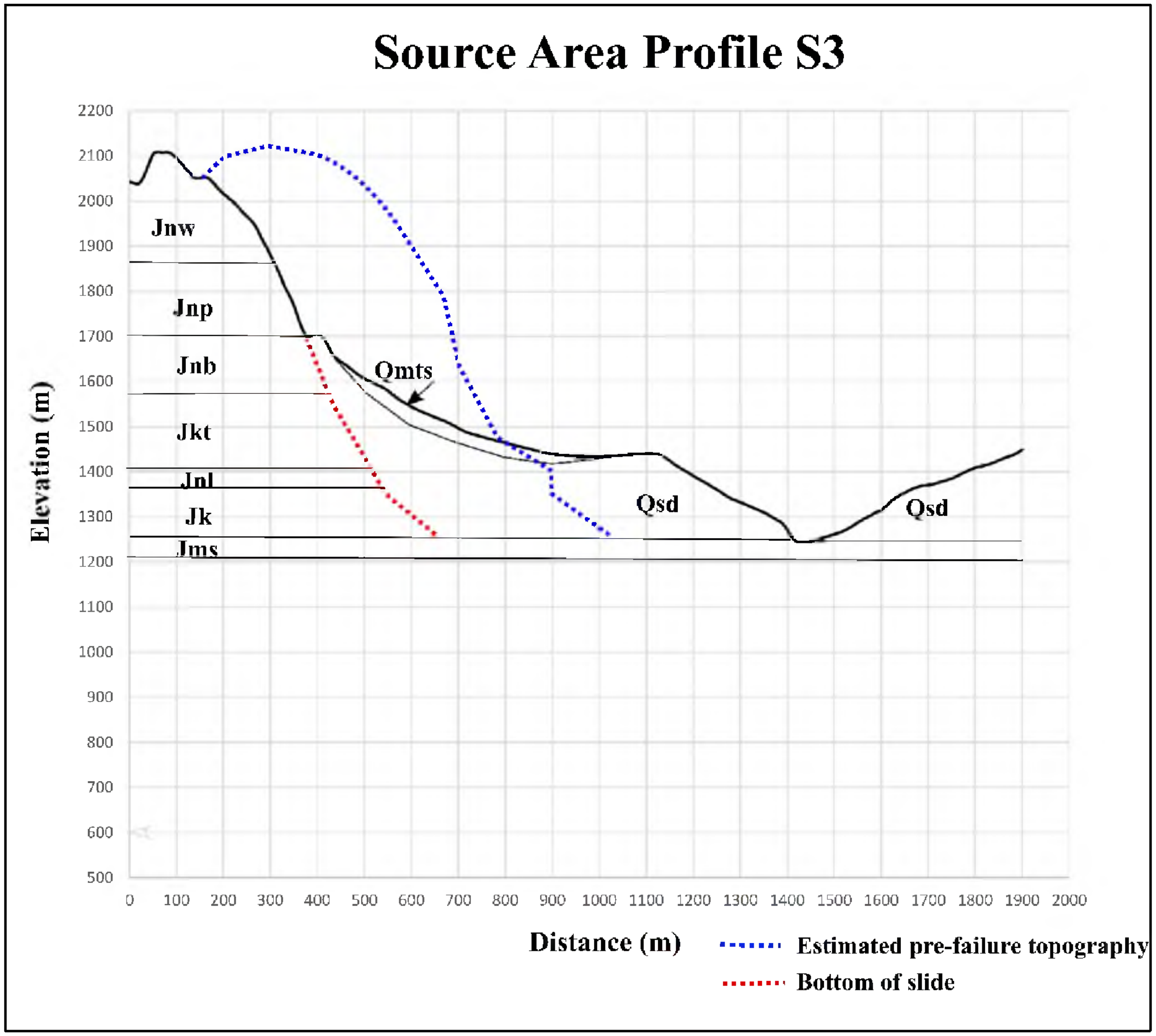


**Figure 31.** Cross section S3.

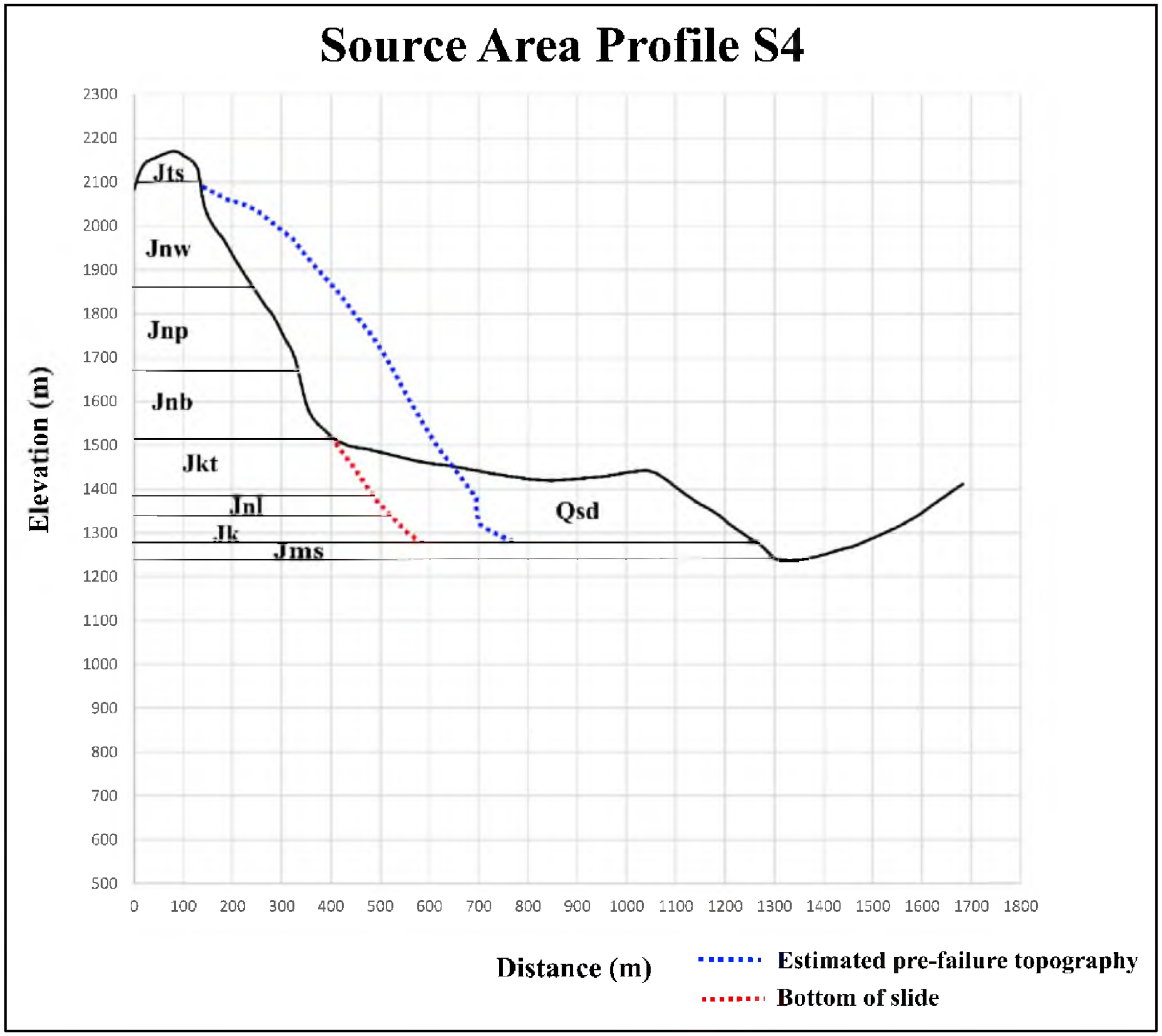


**Figure 32.** Cross section S4.

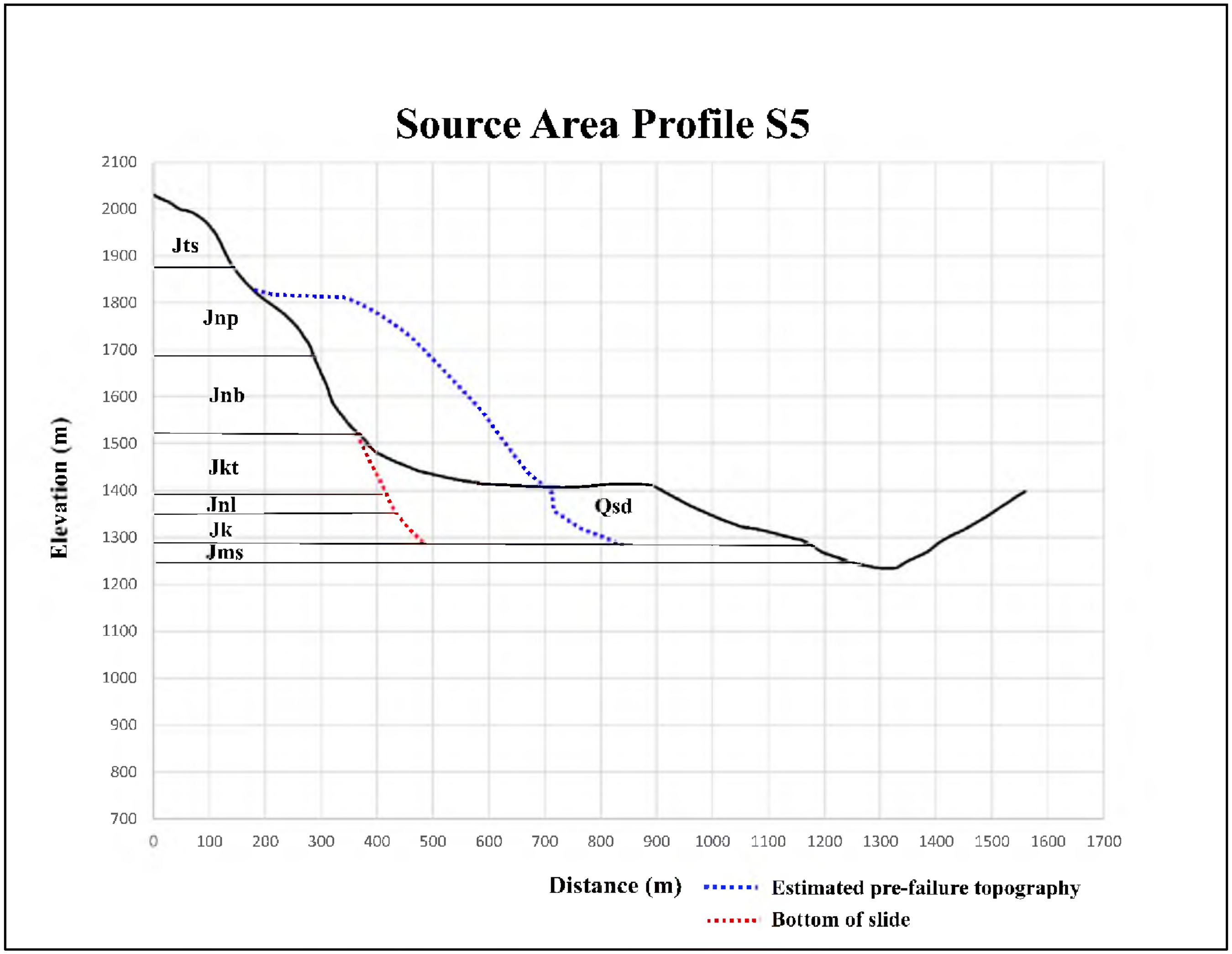


**Figure 33.** Cross section S5.

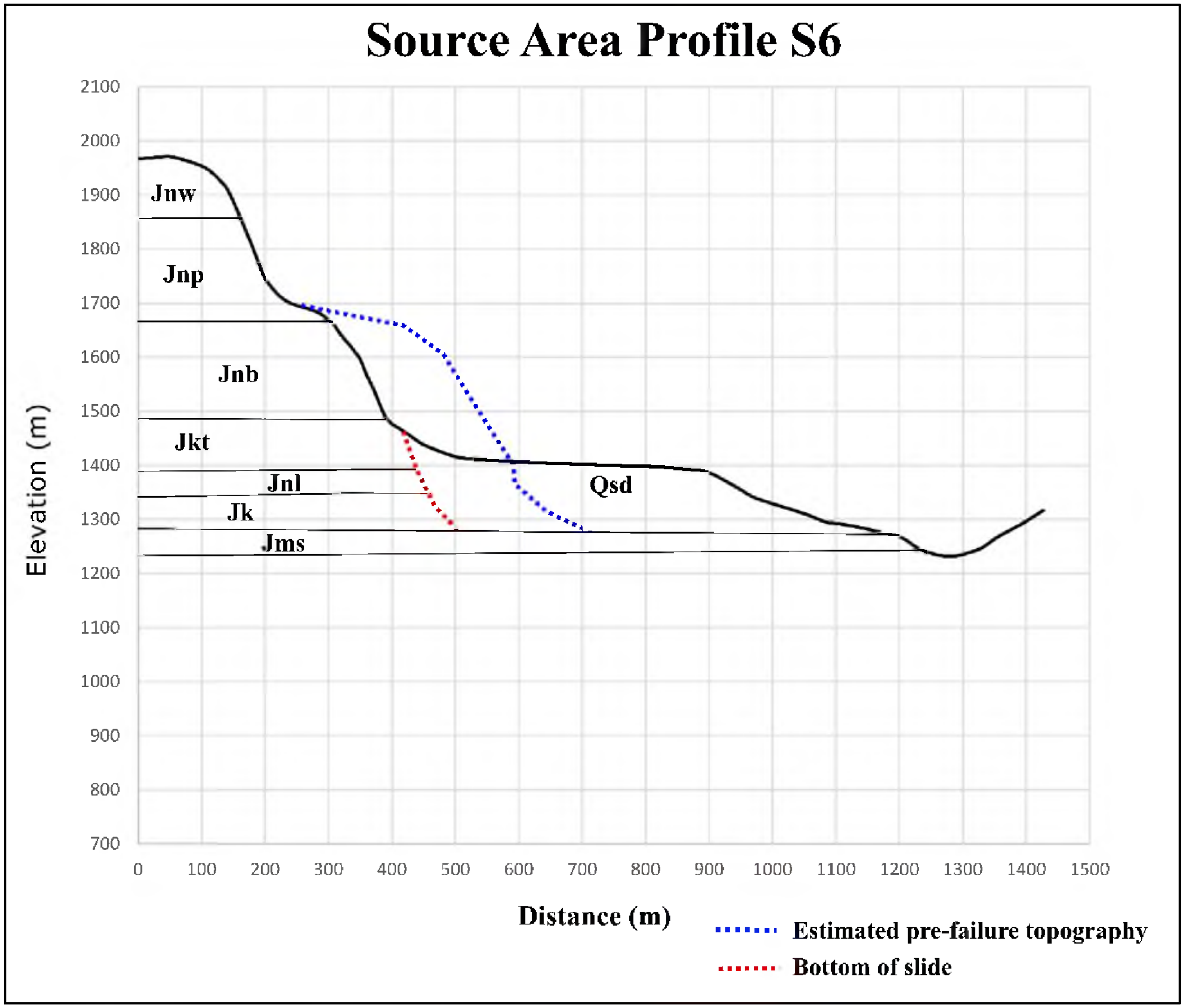


**Figure 34.** Cross section S6.

# APPENDIX B

# SAMPLE DATA

a

b

**Figure 35.** Sample ZCS-1 parameters: Location: 37° 13′ 58.4986″, -112° 57′ 55.2195″; Elevation: 1366m (gaps) 1386.64m (DEM); Lithology: Navajo Sandstone; Boulder Size: Length: 10m, Width: 5.5m, Height: 3m; Strike (°): S 28° W, Dip (°): 8° W; Average Sample Depth: 1.5cm.

a) Photograph of boulder sampled for ZCS-1. b) Photograph of sample size and tools used.


**Figure 36.** Photograph of boulder for sample ZCS-2.

Sample ZCS-2 parameters: Location: 37° 14′ 04.5143″, -112° 57′ 56.002″; Elevation: 1368m (GPS) 1382.12m (DEM); Lithology: Navajo Sandstone (white member); Boulder Size: Length: 6m, Width: 2.5m, Height: 2.75m; Strike (°): N 52° E, Dip (°): 24° SE; Average Sample Depth: 1.5cm.

a

b

**Figure 37.** Sample ZCS-3 parameters: Location: 37° 13′ 52.6990″, -112° 58′ 10.4827″; Elevation: 1417m (GPS) 1437.73m (DEM); Lithology: Navajo Sandstone; Boulder Size: Length: 3m, Width: 2.3m, Height: 1m; Strike (°): S 66° W, Dip (°): 27° N; Average Sample Depth: 1.75cm. a) Photograph of boulder samples for ZCS-3.

b) Photograph of boulder after sample extraction.

a

b

**Figure 38.** Sample ZCS-4 parameters: Location: 37° 13′ 30.8924″, -112° 58′ 34.0682″; Elevation: 1374m (GPS) 1398.12m (DEM); Lithology: Navajo Sandstone (white member); Boulder Size: Length: 15m, Width: 6m, Height: 4.1m; Strike (°): S 10° W, Dip (°): 5° SW; Average Sample Depth: 2cm. a) Photograph of boulder sampled for ZCS-4. b) Photograph of surface samples for ZCS-4.

a

b

**Figure 39.** Sample ZCS-5 parameters: Location: 37° 13′ 22.9455″, -112° 58′ 37.1357″; Elevation: 1367m (GPS), 1387.16m (DEM); Lithology: Navajo Sandstone; Boulder Size: Length: 10.2m, Width: 9m, Height: 4.1m; Strike (°): S 75° W, Dip (°): 16° N; Average Sample Depth: 1.5cm. a) Photograph of boulder sampled for ZCS-5.

b) Photograph of boulder after extraction of sample ZCS-5.


a

b

**Figure 40.** Sample ZCS-6 parameters: Location: 37° 13′ 26.0295″, -112° 58′ 34.9233″; Elevation: 1370m (GPS), 1388.88(DEM); Lithology: Navajo Sandstone; Boulder Size: Length: 12m, Width: 9.7m, Height: 4.2m; Strike (°): S 65° E, Dip (°): 4.5° SE; Average Sample Depth: 2cm. a) Photograph of boulder sampled for ZCS-6. b) Photograph of boulder after extraction of ZCS-6.

a

b

**Figure 41.** ZCS-7 Location: 37° 13′ 35.8436″, -112° 58′ 19.6310″; Elevation: 1415m (GPS), 1434.56m (DEM); Lithology: Navajo Sandstone (white member); Boulder Size: Length: 15m, Width: 10m, Height: 3m; Strike (°): S 3° E, Dip (°): 20° W; Average Sample Depth: 1.75cm. a) Photograph of boulder sampled for ZCS-7. b) Photograph of boulder after extraction of ZCS-7.

a

b

**Figure 42.** Sample ZCS-8 parameters: Location: 37° 13′ 39.3773″, -112° 58′ 16.3099″; Elevation: 1417m (GPS), 1440.18m (DEM); Lithology: Navajo Sandstone (white member); Boulder Size: Length: 5.2m, Width: 3m, Height: 1.2m; Strike (°): N 71° E, Dip (°): 10° SE; Average Sample Depth: 1.5cm. a) Photograph of boulder sampled for ZCS-8. b) Photograph of boulder after extraction of ZCS-8.

a

b

**Figure 43.** ZCS-9a Location: 37° 13′ 51.7431″, -112° 57′ 59.3890″; Elevation: 1386m (GPS), 1400.36m (DEM); Lithology: Navajo Sandstone; Boulder Size: Length: 12m, Width:  8m, Height: 9m, Strike (°): S 21° E, Dip (°): 5.7° W; Average Sample Depth: 1.5cm. a) Photograph of boulder sampled for ZCS-9a. b) Photograph of boulder after extraction of ZCS-9a.

a

b

**Figure 44.** Sample ZCS-9b parameters: Location: 37° 13′ 52.9571″, -112° 58′ 00.5020″; Elevation: 1383m (GPS), 403.50m (DEM); Lithology: Navajo Sandstone; Boulder Size: Length: 3.8m, Width: 4m, Height: 1.6m; Strike (°): N 01° E, Dip (°): 21° E; Average Sample Depth: 1.5cm. a) Photograph of boulder sampled for ZCS-9b. b) Photograph of boulder after extraction of ZCS-9b.

a

b

**Figure 45.** Sample ZCS-10a parameters: Location: 37° 13′ 09.6578″, -112° 58′ 20.0677″; Elevation: 1271m (GPS), 1291.40m (DEM); Lithology: Probably Navajo Sandstone, possible Temple Cap; Boulder Size: Length: 6m, Width: 4m, Height: 2m; Strike (°): S 68° E, Dip(°): 18° S; Average Sample Depth: 1.75cm. a) Photograph of boulder sampled for ZCS-10a. b) Photograph of boulder after extraction of ZCS-10a.

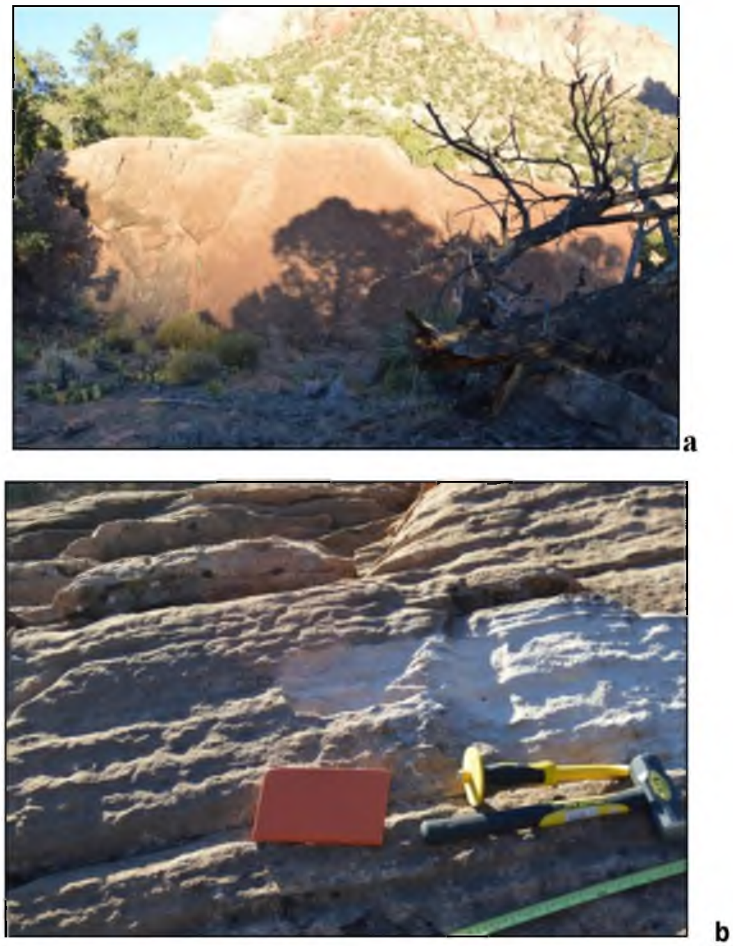


**Figure 46.** Sample ZCS-10b parameters: Location: 37° 13′ 07.3469″, -112° 58′ 21.3041″; Elevation: 1263m (GPS), 1282.80m (DEM); Lithology: Navajo Sandstone (white member), Possible contact on boulder with Temple Cap or Pink Navajo; Boulder Size: Length: 16m, Width: 7.5m, Height: 5m; Strike (°): N 10° E, Dip(°): 3° E; Average Sample Depth: 2cm. a)Photograph of boulder sampled for ZCS-10b. b) Photograph of boulder after extraction of ZCS-10b.

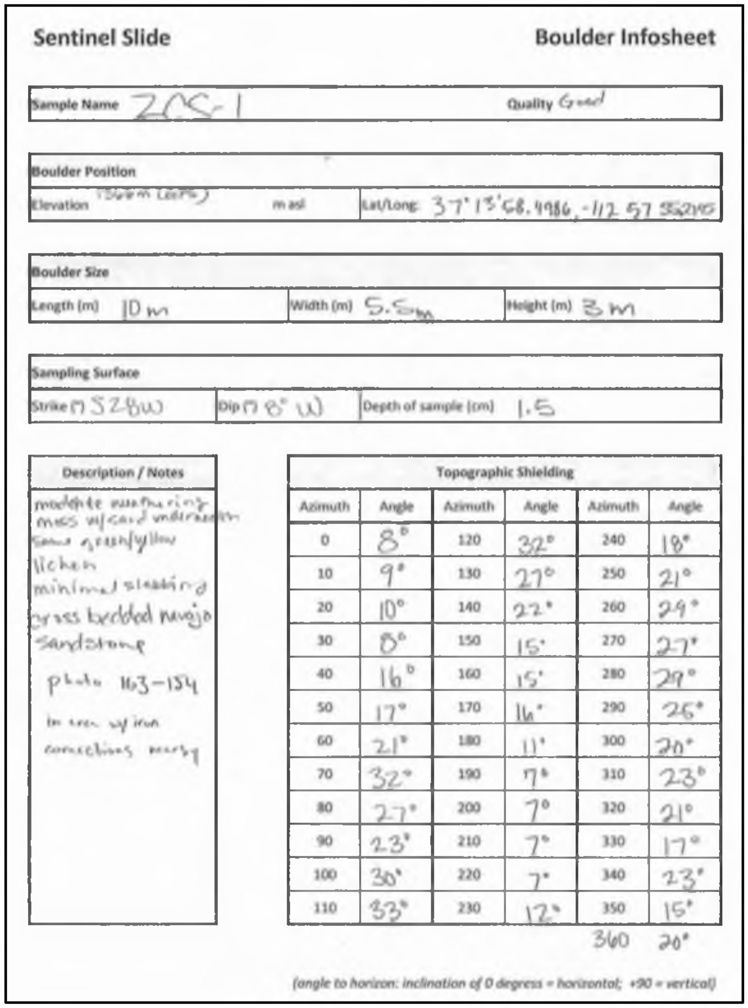

**Sentinel Slide** **Boulder Infosheet**

Sample Name ZCS-1 Quality Good

**Boulder Position**

Elevation 1566 m (GPS) m asl | Lat/Long 37°13'58.4986, -112 57 552195

**Boulder Size**

Length (m) 10 m | Width (m) 5.5 m | Height (m) 3 m

**Sampling Surface**

Strike (°) S28W | Dip (°) 8° W | Depth of sample (cm) 1.5

**Description / Notes**

moderate weathering
moss w/sand underneath
some green/yellow
lichen
minimal sloughing
cross bedded navajo
sandstone

photo 163-154

in area w/ iron
concretions nearby

**Topographic Shielding**

| Azimuth | Angle | Azimuth | Angle | Azimuth | Angle |
|---|---|---|---|---|---|
| 0 | 8° | 120 | 32° | 240 | 18° |
| 10 | 9° | 130 | 27° | 250 | 21° |
| 20 | 10° | 140 | 22° | 260 | 29° |
| 30 | 8° | 150 | 15° | 270 | 27° |
| 40 | 16° | 160 | 15° | 280 | 29° |
| 50 | 17° | 170 | 16° | 290 | 26° |
| 60 | 21° | 180 | 11° | 300 | 20° |
| 70 | 32° | 190 | 17° | 310 | 23° |
| 80 | 27° | 200 | 7° | 320 | 21° |
| 90 | 23° | 210 | 7° | 330 | 17° |
| 100 | 30° | 220 | 7° | 340 | 23° |
| 110 | 33° | 230 | 12° | 350 | 15° |
| | | | | 360 | 20° |

*(angle to horizon: inclination of 0 degrees = horizontal; +90 = vertical)*

**Figure 47.** Sample ZCS-1 field observation sheet.

**Sentinel Slide** **Boulder Infosheet**

| | |
|---|---|
| **Sample Name** ZCS-2 | **Quality** Good + |

| **Boulder Position** | |
|---|---|
| **Elevation** 1360 (GPS) m asl | **Lat/Long:** 37 14 04.5143, -112 57 56.002 |

| **Boulder Size** | | |
|---|---|---|
| **Length (m)** 6m | **Width (m)** 2.5m | **Height (m)** 2.75m |

| **Sampling Surface** | | |
|---|---|---|
| **Strike (°)** N52E | **Dip (°)** 24° SE | **Depth of sample (cm)** 1-2.5 (1.5-2) 1.5 |

**Description / Notes**

Pic 164–167

hard rock (harder than ZCS-1)

mazanita tree growing in fracture

some black lichen

yellow, green lichen

dark weathered old surface next to lighter fresher surface

Kayenta (?)

Soft sediment deformation

hard to chip out

**Topographic Shielding**

| Azimuth | Angle | Azimuth | Angle | Azimuth | Angle |
|---|---|---|---|---|---|
| 0 | 19° | 120 | 27° | 240 | 16° |
| 10 | 5° | 130 | 29° | 250 | 21° |
| 20 | 5° | 140 | 28° | 260 | 29° |
| 30 | 6° | 150 | 15° | 270 | 29° |
| 40 | 13° | 160 | 13° | 280 | 26° |
| 50 | 16° | 170 | 12° | 290 | 17° |
| 60 | 19° | 180 | 14° | 300 | 25° |
| 70 | 22° | 190 | 12° | 310 | 21° |
| 80 | 20° | 200 | 5° | 320 | 18° |
| 90 | 28° | 210 | 4° | 330 | 25° |
| 100 | 32° | 220 | 4° | 340 | 27° |
| 110 | 24° | 230 | 4° | 350 | 15° |

*(angle to horizon: inclination of 0 degress = horizontal; +90 = vertical)*

**Figure 48.** Sample ZCS-2 field observation sheet.

**Sentinel Slide** **Boulder Infosheet**

| | |
|---|---|
| Sample Name ZCS-3 | Quality ok to marginal |

| Boulder Position | |
|---|---|
| Elevation 1417 m (GPS) m asl | Lat/Long: 37 13 52.990, 112 58 10.4827 |

| Boulder Size | | |
|---|---|---|
| Length (m) 4 (3) | Width (m) 2.3 | Height (m) 1 m |

| Sampling Surface | | |
|---|---|---|
| Strike (°) S66W | Dip (°) 27° N | Depth of sample (cm) 1.5-2 cm (1.75) |

**Description / Notes**

red sandstone
slabbing
potential for
erosion on
surface
pos. Navajo

very easy to
chip out & cut

Pic 168-173

coarse grains)

old hilltop,
much sand

may have higher
surface erosion rates.

**Topographic Shielding**

| Azimuth | Angle | Azimuth | Angle | Azimuth | Angle |
|---|---|---|---|---|---|
| 0 | 16° | 120 | 21° | 240 | 20° |
| 10 | 10° | 130 | 15° | 250 | 23° |
| 20 | 11° | 140 | 14° | 260 | 28° |
| 30 | 5° | 150 | 11° | 270 | 36° |
| 40 | 10° | 160 | 9° | 280 | 33° |
| 50 | 12° | 170 | 12° | 290 | 35° |
| 60 | 13° | 180 | 5° | 300 | 34° |
| 70 | 19° | 190 | 2° | 310 | 28° |
| 80 | 21° | 200 | 2° | 320 | 24° |
| 90 | 28° | 210 | 2° | 330 | 21° |
| 100 | 20° | 220 | 8° | 340 | 21° |
| 110 | 27° | 230 | 15° | 350 | 22° |

*(angle to horizon: inclination of 0 degress = horizontal; +90 = vertical)*

**Figure 49.** Sample ZCS-3 field observation sheet.

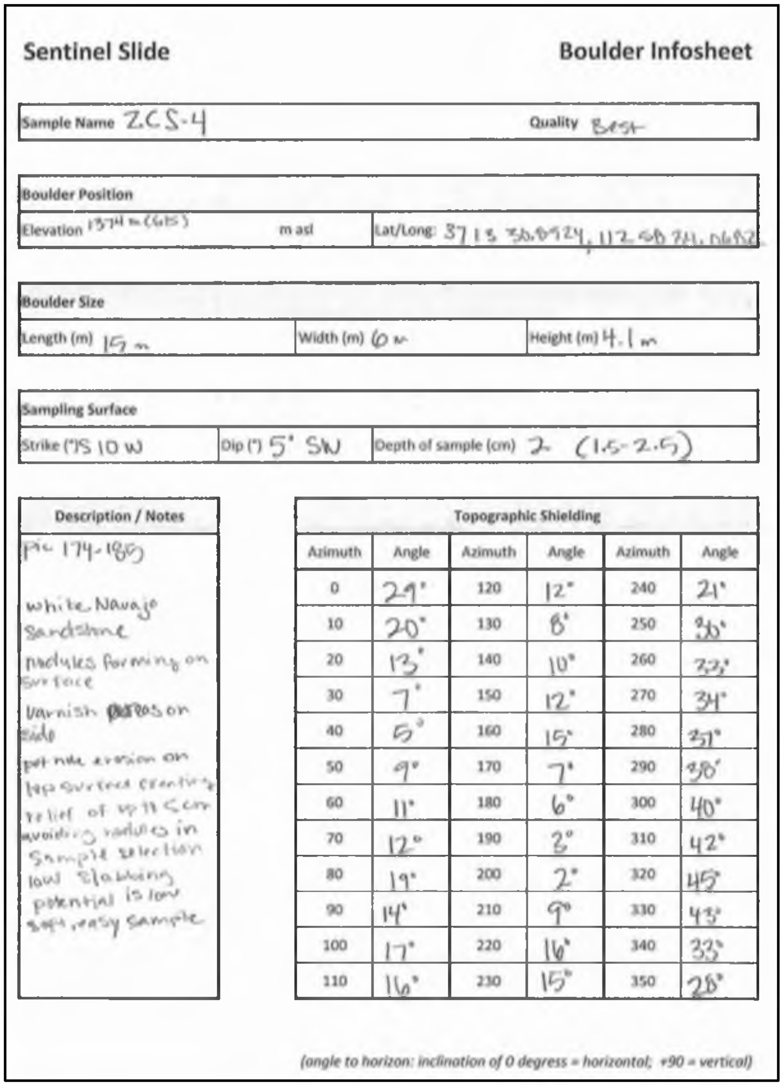

**Sentinel Slide** **Boulder Infosheet**

Sample Name ZCS-4 Quality Best

| Boulder Position | |
|---|---|
| Elevation 1374 m (GPS) m asl | Lat/Long: 37 15 36.0924, 112 58 24.0692 |

| Boulder Size | | |
|---|---|---|
| Length (m) 15 m | Width (m) 6 m | Height (m) 4.1 m |

| Sampling Surface | | |
|---|---|---|
| Strike (°) S 10 W | Dip (°) 5° SW | Depth of sample (cm) 2 (1.5-2.5) |

**Description / Notes**

Pic 174-185

white Navajo sandstone

nodules forming on surface

varnish areas on side

pot hole erosion on top surface creating relief of up to 5 cm

avoiding nodules in sample selection

low slabbing potential is low

soft, easy sample

**Topographic Shielding**

| Azimuth | Angle | Azimuth | Angle | Azimuth | Angle |
|---|---|---|---|---|---|
| 0 | 29° | 120 | 12° | 240 | 21° |
| 10 | 20° | 130 | 8° | 250 | 36° |
| 20 | 13° | 140 | 10° | 260 | 33° |
| 30 | 7° | 150 | 12° | 270 | 34° |
| 40 | 5° | 160 | 15° | 280 | 37° |
| 50 | 9° | 170 | 7° | 290 | 38° |
| 60 | 11° | 180 | 6° | 300 | 40° |
| 70 | 12° | 190 | 3° | 310 | 42° |
| 80 | 19° | 200 | 2° | 320 | 45° |
| 90 | 14° | 210 | 9° | 330 | 43° |
| 100 | 17° | 220 | 16° | 340 | 33° |
| 110 | 16° | 230 | 15° | 350 | 28° |

*(angle to horizon: inclination of 0 degress = horizontal; +90 = vertical)*

**Figure 50.** Sample ZCS-4 field observation sheet.

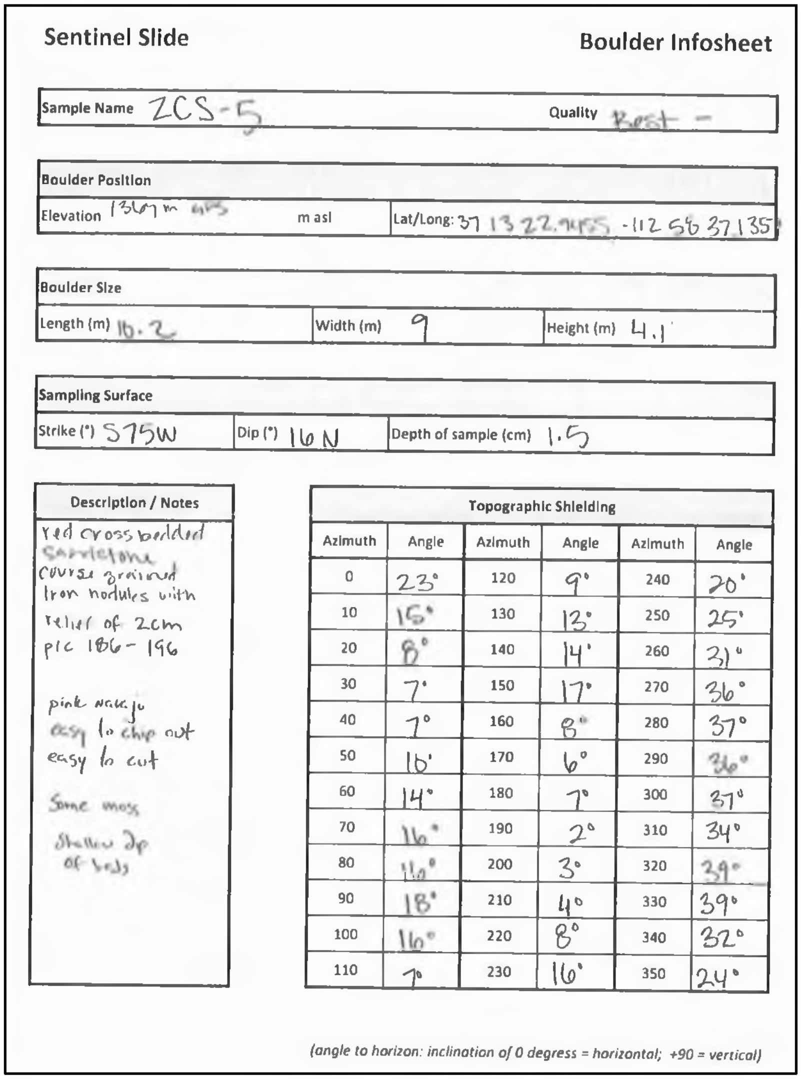

Sentinel Slide

Boulder Infosheet

Sample Name ZCS-5 Quality Best -

**Boulder Position**

Elevation 1369 m GPS m asl | Lat/Long: 37 13 22.9455 -112 58 37.135

**Boulder Size**

Length (m) 16.2 | Width (m) 9 | Height (m) 4.1

**Sampling Surface**

Strike (°) S75W | Dip (°) 16 N | Depth of sample (cm) 1.5

**Description / Notes**

red cross bedded
sandstone
course grained
Iron nodules with
relief of 2cm
pic 186 - 196

pink navajo
easy to chip out
easy to cut

Some moss

Shallow dip
of beds

**Topographic Shielding**

| Azimuth | Angle | Azimuth | Angle | Azimuth | Angle |
|---|---|---|---|---|---|
| 0 | 23° | 120 | 9° | 240 | 20° |
| 10 | 15° | 130 | 13° | 250 | 25° |
| 20 | 8° | 140 | 14° | 260 | 31° |
| 30 | 7° | 150 | 17° | 270 | 36° |
| 40 | 7° | 160 | 8° | 280 | 37° |
| 50 | 16° | 170 | 6° | 290 | 36° |
| 60 | 14° | 180 | 7° | 300 | 37° |
| 70 | 16° | 190 | 2° | 310 | 34° |
| 80 | 16° | 200 | 3° | 320 | 39° |
| 90 | 18° | 210 | 4° | 330 | 39° |
| 100 | 16° | 220 | 8° | 340 | 32° |
| 110 | 7° | 230 | 16° | 350 | 24° |

*(angle to horizon: inclination of 0 degress = horizontal; +90 = vertical)*

**Figure 51.** Sample ZCS-5 field observation sheet.

**Sentinel Slide** **Boulder Infosheet**

**Sample Name** ZCS-6 **Quality** Good +

**Boulder Position**

**Elevation** 1870 m m asl **Lat/Long:** 37 13 26.0296, -112 58 31.0323

**Boulder Size**

**Length (m)** 12 m **Width (m)** 9.7 m **Height (m)** 4.2

**Sampling Surface**

**Strike (°)** 3 65 E **Dip (°)** 4.5° SE **Depth of sample (cm)** 2 cm

**Description / Notes**

pic 202 - 206

crossbedded, course, sandstone Navajo

2 cm relief caused by vertical cross bedding

not as old looking as others on surface

slightly harder to chip out, pos. due to vert. bedding

**Topographic Shielding**

| Azimuth | Angle | Azimuth | Angle | Azimuth | Angle |
|---|---|---|---|---|---|
| 0 | 21° | 120 | 7° | 240 | 20° |
| 10 | 13° | 130 | 9° | 250 | 29° |
| 20 | 8° | 140 | 12° | 260 | 33° |
| 30 | 7° | 150 | 16° | 270 | 34° |
| 40 | 10° | 160 | 12° | 280 | 35° |
| 50 | 14° | 170 | 6° | 290 | 37° |
| 60 | 16° | 180 | 7° | 300 | 36° |
| 70 | 13° | 190 | 3° | 310 | 38° |
| 80 | 19° | 200 | 3° | 320 | 40° |
| 90 | 13° | 210 | 4° | 330 | 40° |
| 100 | 18° | 220 | 14° | 340 | 35° |
| 110 | 17° | 230 | 19° | 350 | 26° |

*(angle to horizon: inclination of 0 degress = horizontal; +90 = vertical)*

**Figure 52.** Sample ZCS-6 field observation sheet.

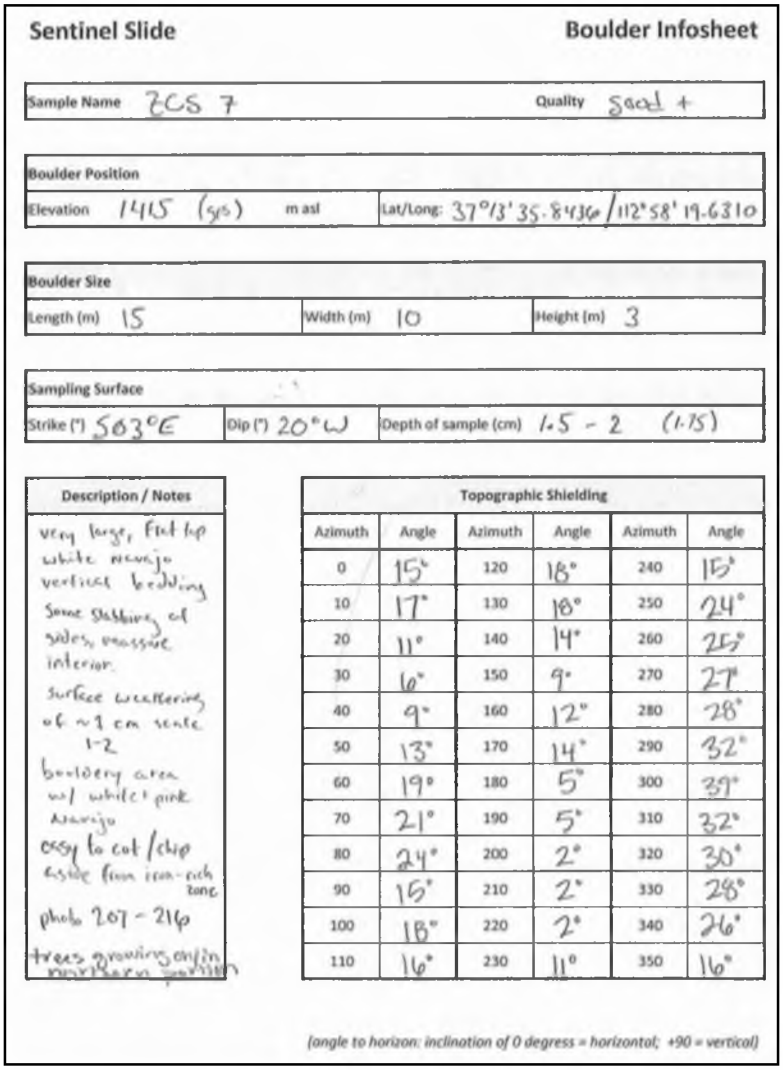

Sentinel Slide

Boulder Infosheet

| | |
|---|---|
| Sample Name ZCS 7 | Quality good + |

| Boulder Position | |
|---|---|
| Elevation 1415 (gps) m asl | Lat/Long: 37°13' 35.8436 / 112°58' 19.6310 |

| Boulder Size | | |
|---|---|---|
| Length (m) 15 | Width (m) 10 | Height (m) 3 |

| Sampling Surface | | |
|---|---|---|
| Strike (°) S63°E | Dip (°) 20°W | Depth of sample (cm) 1.5 - 2 (1.75) |

Description / Notes

very large, flat top
white navajo
vertical bedding
Some slabbing of
sides, massive
interior
surface weathering
of ~1 cm scale
1-2
bouldery area
w/ white + pink
Navajo
easy to cut / chip
aside from iron-rich
zone
photo 207 - 216
trees growing on/in
northern portion

Topographic Shielding

| Azimuth | Angle | Azimuth | Angle | Azimuth | Angle |
|---|---|---|---|---|---|
| 0 | 15° | 120 | 18° | 240 | 15° |
| 10 | 17° | 130 | 18° | 250 | 24° |
| 20 | 11° | 140 | 14° | 260 | 25° |
| 30 | 6° | 150 | 9° | 270 | 27° |
| 40 | 9° | 160 | 12° | 280 | 28° |
| 50 | 13° | 170 | 14° | 290 | 32° |
| 60 | 19° | 180 | 5° | 300 | 37° |
| 70 | 21° | 190 | 5° | 310 | 32° |
| 80 | 24° | 200 | 2° | 320 | 30° |
| 90 | 15° | 210 | 2° | 330 | 28° |
| 100 | 18° | 220 | 2° | 340 | 26° |
| 110 | 16° | 230 | 11° | 350 | 16° |

(angle to horizon: inclination of 0 degress = horizontal; +90 = vertical)

**Figure 53.** Sample ZCS-7 field observation sheet.

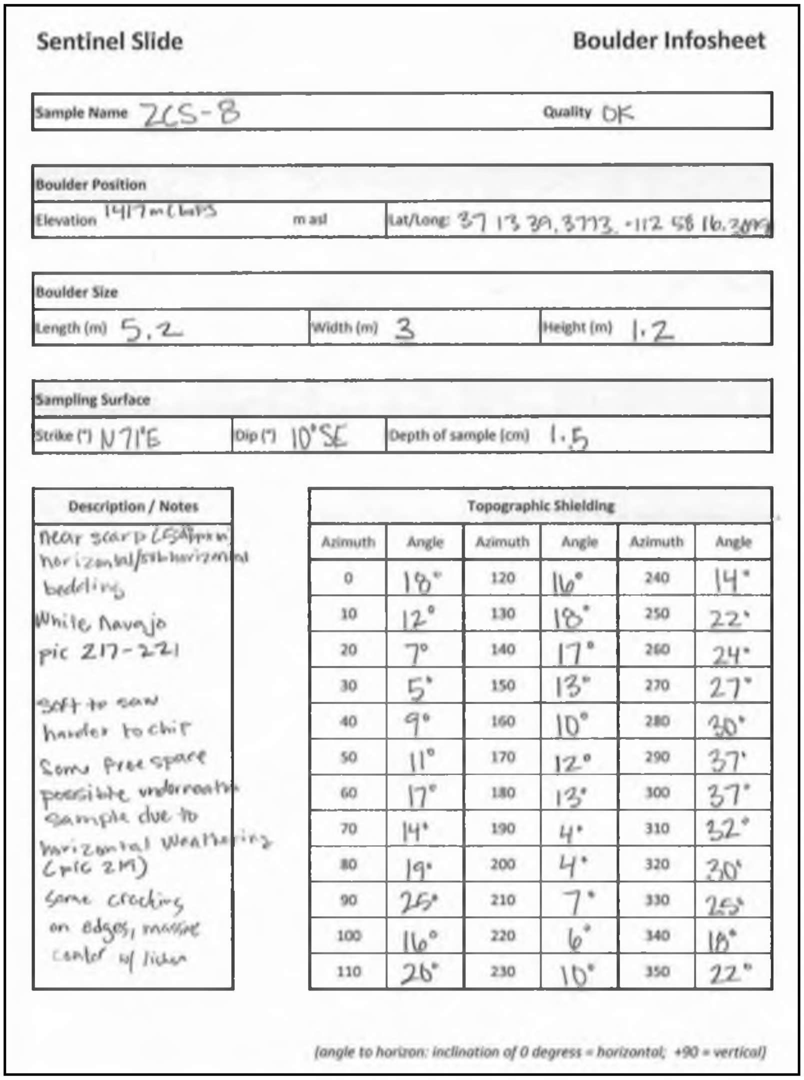

**Sentinel Slide** **Boulder Infosheet**

Sample Name ZCS-8 Quality OK

**Boulder Position**

Elevation 1417 m (GPS m asl | Lat/Long: 37 13 39.3773, -112 58 16.2[illegible]

**Boulder Size**

Length (m) 5.2 | Width (m) 3 | Height (m) 1.2

**Sampling Surface**

Strike (°) N71°E | Dip (°) 10°SE | Depth of sample (cm) 1.5

**Description / Notes**

near scarp (~5 approx) horizontal/subhorizontal bedding
White Navajo
pic 217-221

Soft to saw
harder to chip
Some free space possible underneath sample due to horizontal weathering (pic 211)
Some cracking on edges, massive center w/ lichen

**Topographic Shielding**

| Azimuth | Angle | Azimuth | Angle | Azimuth | Angle |
|---|---|---|---|---|---|
| 0 | 18° | 120 | 16° | 240 | 14° |
| 10 | 12° | 130 | 18° | 250 | 22° |
| 20 | 7° | 140 | 17° | 260 | 24° |
| 30 | 5° | 150 | 13° | 270 | 27° |
| 40 | 9° | 160 | 10° | 280 | 30° |
| 50 | 11° | 170 | 12° | 290 | 37° |
| 60 | 17° | 180 | 13° | 300 | 37° |
| 70 | 14° | 190 | 4° | 310 | 32° |
| 80 | 19° | 200 | 4° | 320 | 30° |
| 90 | 25° | 210 | 7° | 330 | 25° |
| 100 | 16° | 220 | 6° | 340 | 18° |
| 110 | 26° | 230 | 10° | 350 | 22° |

*(angle to horizon: inclination of 0 degress = horizontal; +90 = vertical)*

**Figure 54.** Sample ZCS-8 field observation sheet.

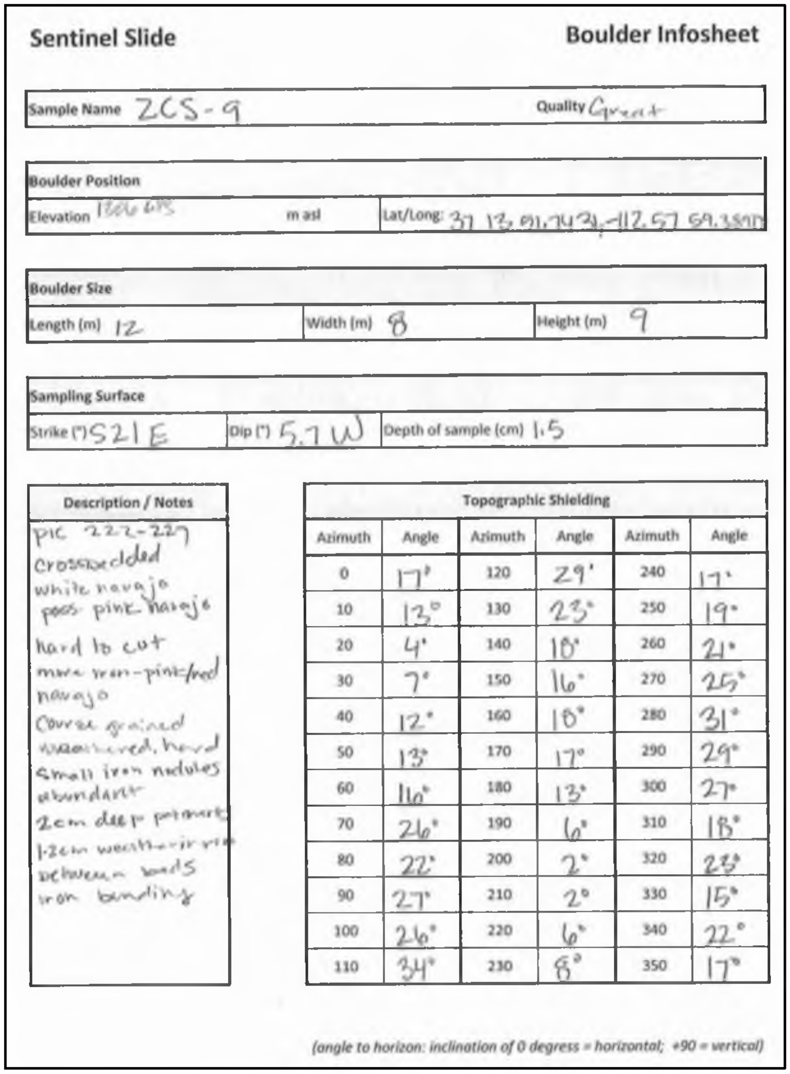

Sentinel Slide

Boulder Infosheet

Sample Name ZCS-9 Quality Great

Boulder Position

Elevation 1806 GPS m asl | Lat/Long: 37 13 01.7434, -112 57 59.3807

Boulder Size

Length (m) 12 | Width (m) 8 | Height (m) 9

Sampling Surface

Strike (°) S21E | Dip (°) 57W | Depth of sample (cm) 1.5

Description / Notes

pic 222-227
crossbedded
white navajo
pass pink navajo
hard to cut
more iron-pink/red
navajo
Course grained
weathered, hard
Small iron nodules
abundant
2cm deep pitmarks
1-2cm weathering rim
between beds
iron banding

Topographic Shielding

| Azimuth | Angle | Azimuth | Angle | Azimuth | Angle |
|---|---|---|---|---|---|
| 0 | 17° | 120 | 29° | 240 | 17° |
| 10 | 13° | 130 | 23° | 250 | 19° |
| 20 | 4° | 140 | 18° | 260 | 21° |
| 30 | 7° | 150 | 16° | 270 | 25° |
| 40 | 12° | 160 | 18° | 280 | 31° |
| 50 | 13° | 170 | 17° | 290 | 29° |
| 60 | 16° | 180 | 13° | 300 | 27° |
| 70 | 26° | 190 | 6° | 310 | 18° |
| 80 | 22° | 200 | 2° | 320 | 23° |
| 90 | 27° | 210 | 2° | 330 | 15° |
| 100 | 26° | 220 | 6° | 340 | 22° |
| 110 | 34° | 230 | 8° | 350 | 17° |

*(angle to horizon: inclination of 0 degress = horizontal; +90 = vertical)*

**Figure 55.** Sample ZCS-9a field observation sheet.

**Sentinel Slide** | **Boulder Infosheet**

| | |
|---|---|
| Sample Name: ZCS- 9b | Quality: marginal |

| Boulder Position | |
|---|---|
| Elevation: 1383 (gps) m asl | Lat/Long: 37°13'52.957N / 112°58'00.5020 |

| Boulder Size | | |
|---|---|---|
| Length (m): 3.8 | Width (m): 4 | Height (m): 1.6 |

| Sampling Surface | | |
|---|---|---|
| Strike (°): N01°E | Dip (°): 21°E | Depth of sample (cm): 1.5 |

**Description / Notes**

white Navajo gently dipping bedding weathered surface friable some slabbing near sample ZCS-9 (30m away) White navajo ss here is weathered thick brush around, surface clear photo 228-232

**Topographic Shielding**

| Azimuth | Angle | Azimuth | Angle | Azimuth | Angle |
|---|---|---|---|---|---|
| 0 | 14° | 120 | 31° | 240 | 14° |
| 10 | 18° | 130 | 23° | 250 | 18° |
| 20 | 12° | 140 | 18° | 260 | 21° |
| 30 | 4° | 150 | 16° | 270 | 31° |
| 40 | 6° | 160 | 17° | 280 | 30° |
| 50 | 11° | 170 | 16° | 290 | 30° |
| 60 | 15° | 180 | 13° | 300 | 27° |
| 70 | 17° | 190 | 14° | 310 | 18° |
| 80 | 27° | 200 | 8° | 320 | 20° |
| 90 | 20° | 210 | 7° | 330 | 21° |
| 100 | 26° | 220 | 7° | 340 | 23° |
| 110 | 27° | 230 | 8° | 350 | 17° |

*(angle to horizon: inclination of 0 degress = horizontal; +90 = vertical)*

**Figure 56.** Sample ZCS-9b field observation sheet.

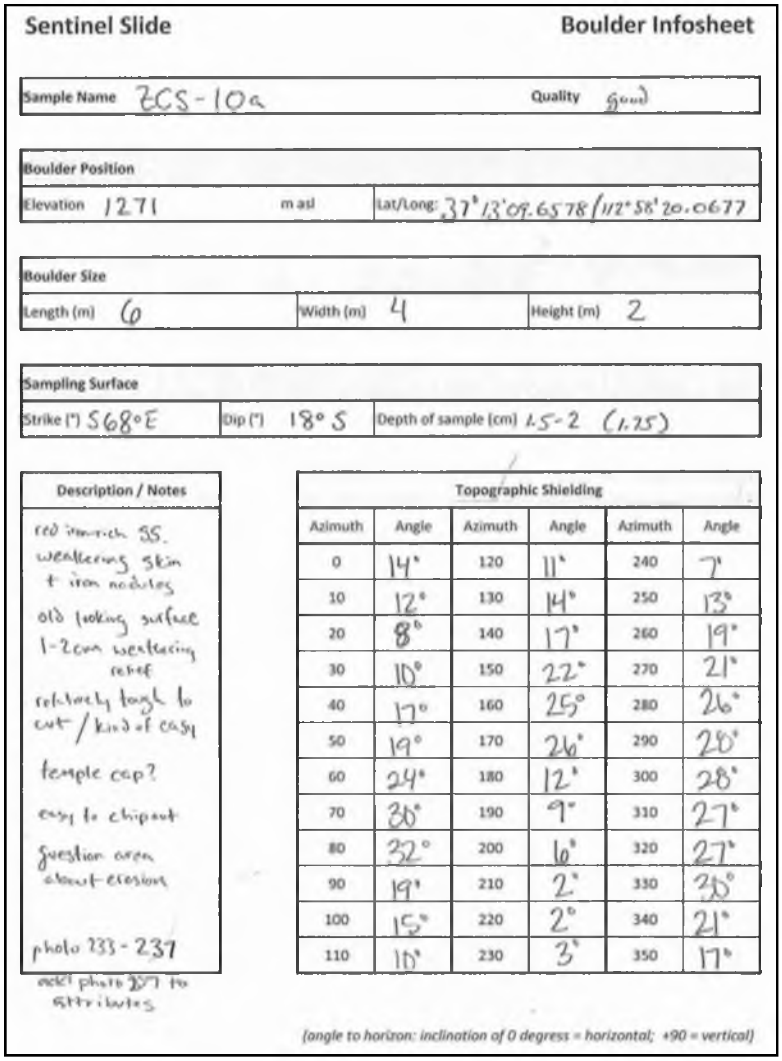

**Sentinel Slide** **Boulder Infosheet**

| Sample Name | ZCS-10a | Quality | good |
|---|---|---|---|

| Boulder Position | | | |
|---|---|---|---|
| Elevation | 1271 m asl | Lat/Long: | 37°13'09.6578/112°58'20.0677 |

| Boulder Size | | | | | |
|---|---|---|---|---|---|
| Length (m) | 6 | Width (m) | 4 | Height (m) | 2 |

| Sampling Surface | | | | | |
|---|---|---|---|---|---|
| Strike (°) | S68°E | Dip (°) | 18° S | Depth of sample (cm) | 1.5-2 (1.25) |

**Description / Notes**

red iron-rich SS.
weathering skin
+ iron nodules

old looking surface
1-2cm weathering
relief

relatively tough to
cut / kind of easy

temple cap?

easy to chip out

question area
about erosion

photo 233-237

add'l photo 237 to
attributes

**Topographic Shielding**

| Azimuth | Angle | Azimuth | Angle | Azimuth | Angle |
|---|---|---|---|---|---|
| 0 | 14° | 120 | 11° | 240 | 7° |
| 10 | 12° | 130 | 14° | 250 | 13° |
| 20 | 8° | 140 | 17° | 260 | 19° |
| 30 | 10° | 150 | 22° | 270 | 21° |
| 40 | 17° | 160 | 25° | 280 | 26° |
| 50 | 19° | 170 | 26° | 290 | 28° |
| 60 | 24° | 180 | 12° | 300 | 28° |
| 70 | 30° | 190 | 9° | 310 | 27° |
| 80 | 32° | 200 | 6° | 320 | 27° |
| 90 | 19° | 210 | 2° | 330 | 35° |
| 100 | 15° | 220 | 2° | 340 | 21° |
| 110 | 10° | 230 | 3° | 350 | 17° |

*(angle to horizon: inclination of 0 degress = horizontal; +90 = vertical)*

**Figure 57.** Sample ZCS-10a field observation sheet.

**Sentinel Slide** **Boulder Infosheet**

| | |
|---|---|
| **Sample Name** ZCS-10b | **Quality** Good |

| **Boulder Position** | |
|---|---|
| **Elevation** 1263 GPS m asl | **Lat/Long:** 37 13 07.3469, -112 58 21.3841 |

| **Boulder Size** | | |
|---|---|---|
| **Length (m)** 16 | **Width (m)** 7.5 | **Height (m)** 5 |

| **Sampling Surface** | | |
|---|---|---|
| **Strike (°)** N10°E | **Dip (°)** 3°E | **Depth of sample (cm)** 2 |

**Description / Notes**

pic 238-247
Crossbedded white navajo some small iron concretions possible contact w/ temple cap red sandstone finer grained easy cutting moderate chipping effort

**Topographic Shielding**

| Azimuth | Angle | Azimuth | Angle | Azimuth | Angle |
|---|---|---|---|---|---|
| 0 | 14° | 120 | 14° | 240 | 8° |
| 10 | 12° | 130 | 22° | 250 | 12° |
| 20 | 8° | 140 | 26° | 260 | 16° |
| 30 | 12° | 150 | 28° | 270 | 23° |
| 40 | 16° | 160 | 26° | 280 | 23° |
| 50 | 17° | 170 | 13° | 290 | 29° |
| 60 | 23° | 180 | 8° | 300 | 29° |
| 70 | 28° | 190 | 9° | 310 | 27° |
| 80 | 25° | 200 | 3° | 320 | 24° |
| 90 | 19° | 210 | 2° | 330 | 27° |
| 100 | 8° | 220 | 2° | 340 | 21° |
| 110 | 11° | 230 | 7° | 350 | 14° |

*(angle to horizon: inclination of 0 degress = horizontal; +90 = vertical)*

**Figure 58.** Sample ZCS-10b field observation sheet.

## REFERENCES


Balco, G., Stone, J.O., Lifton, N.A., Dunal, T.J., 2008, A complete and easily accessible means of calculating surface exposure ages or erosion rates from 10Be and 26Al measurements, Quaternary Geochronology, vol. 3 pp. 174-195.

Balco, G., Briner, J., Finkel, R.C., Rayburn, J.A., Ridge, J.C., Schaefer, J.M., 2009, Regional beryllium-10 production rate calibrations for late-glacial northeastern North America, Quaternary Geology, vol. 4, pp. 93-107, doi: 10.1016/j.quageo.2008.09.001.

Balco, G., 2011, Contributions and unrealized potential contributions of cosmogenic-nuclide exposure dating to glacier chronology, 1990-2010, Quaternary Science Reviews, vol. 30, no. 1-2, pp. 3-27.

Barth, N.C., 2013, The Cascade rock avalanche: implications of a very large Alpine Fault-triggered failure, New Zealand, Landslides, 15 p., doi: 10.1007/s10346-013-0389-1.

Biek, R.F., Willis, G.C., Hylland, M.D., Doelling, H.H., 2012, Geologic road guides to Zion National Park, Utah: Geologic road, trail, and lake guides to Utah's Parks and Monuments (third edition), P.B. Anderson and D.A. Sprinkel, editors, Utah Geological Association Publication 29, 89 p.

Biek, R.F., Willis, G.C., Hylland, M.D., Doelling, H.H., 2003, Geology of Zion National Park, in Sprinkel, D.A., Geologic hazards of the Zions National Park geologic-hazard study area, Washington and Kane Counties, Utah 13, Chidsey, T.C., Jr., and Anderson, P.B., editors, Geology of Utah's parks and monuments (second edition): Utah Geological Association Publication 28, p.106-137.

Biek, R.F., Willis, G.C., Hylland, M.D., Doelling, H.H., 2000, Geology of Zion National Park, Utah, in D.A. Sprinkel, T.C. Chidsey, Jr., and P.B. Anderson, editors., Geology of Utah's Parks and Monuments: Utah Geological Association Publication 28, p. 107- 138.

Bourruer, F., Dorren, L., Hungr, O., 2013, The use of ballistic trajectory and granular flow models in predicting rockfall propagation, Earth Surface Processes and Landforms, vol. 34, no. 4, pp. 435-430, doi: 10.1002/esp.3372.

Crosta, G. B., Frattini, P., Fusi, N., 2007, Fragmentation in the Val Pola rock avalanche, Italian Alps. Journal of Geophysical Research, 112, F01006. doi:http://dx.doi.org/10.1029/2005JF000455

Davies, T.R., McSaveney, M.J., 2002, Dynamic simulation of the motion of fragmenting rock avalanches, Canadian Geotechnical Journal, vol. 39, pp. 789-798, doi: 10.1139/T02-035.

Deline, P., Alberto, W., Broccolato, M., Hungr, O., Noetzli, J., Tamburini, A., 2011, The December 2008 Crammont rock avalanche, Mont Blanc massif area, Italy, Natural Hazards and Earth System Sciences, vol. 11, p. 3307-3318, doi 10.5194/nhess-11-3307-2011.

Doelling, H.H., Willis, G.C., Solomon, B.J., Sable, E.G., Hamilton, W.L., Naylor, L.P. II., 2002, Interim Geologic Map of the Springdale East Quadrangle, Washington County, Utah, Utah Geological Survey Open File-Report 393, 23 p.

Friedmann, S.J., 1997, Rock-avalanche elements of the Shadow Valley Basin Eastern Mojave Desert, California: processes and problems, Journal of Sedimentary Research, vol. 67, no. , pp. 792-804.

Graham, J., 2006, Zion National Park Geologic Resource Evaluation Report. Natural Resource Report NPS/NRPC/GRD/NRR—2006/014. National Park Service, Denver, Colorado.

Grater, R.K., 1945, Landslide in Zion Canyon, Zion National Park, Utah, Journal of Geology, 43, 116-124.

Hamilton, W.L., 2014, Ancient lakes of Zion National Park, in MacLean, J.S., Biek, R.F., Huntoon, J.E., editors, Geology of Utah's Far South, Utah Geological Association Publication 43, pp. 1-23.

Hamilton, W.L., 1984 (revised 1992, 1995, and 2004), The sculpturing of Zion, with road guide to the geology of Zion National Park: Zion Natural History Association, 132 p.

Hamilton, W.L., 1976, Holocene and Pleistocene lakes in Zion National Park, Utah, Proceedings of the First Conference on Scientific Research in the National Parks, New Orleans, LA.

Hungr, O., Evans, 2004, Entrainment of debris in rock avalanches: an analysis of a long run-out mechanism, GSA Bulletin, September/October 2004, vol. 116, no. 9/10, pp. 1240-1252; doi: 10.1130/B25362.1.

Hungr, O., Evans, S.G., Bovis, M.J., Hutchinson, J.N., 2001, A Review of the Classification of Landslides of the Flow Type. – Environmental & Engineering Geoscience, VII–3, 221–238.

Hungr, O., Evans, S.G., 1996, Rock avalanche runout prediction using a dynamic model, In Proceedings of the 7th International Symposium on Landslides, Trondheim, Norway, Vol. 17, p. 21.

Hungr, O. 1995. A model for the analysis of rapid flow slides, debris flows, and avalanches, Canadian Geotechnical Journal vol. 32, no. 4 pp. 610-623.

Ivy-Ochs, S., Kober, F., 2008, Surface exposure dating with cosmogenic nuclides, Eiszeitalter and Gegenwart Quaternary Science Journal, 57/1-2, pp. 179-209.

Ivy-Ochs, S., Poschinger, A.V., Synal, H.A., Maisch, M., 2009, Surface exposure dating of the Flims rockslide, Graubünden, Switzerland. Geomorphology 103. p. 104-112.

Knudsen, T.R., Lund, W.R., 2013, Geologic hazards of the State Route 9 corridor, La Verkin City to town of Springdale, Washington County, Utah, Utah Geological Survey, Special Study 148, 13 p.

Lal, D., 1991, Cosmic ray labeling of erosion surfaces: in-situ nuclide production rates and erosion models, Earth and Planetary Science Letters, 104: 424-439.

Lund, W.R., Hozik, M.J., Hatfield, S.C., 2007, Paleoseismic investigation and long-term slip history of the Hurricane fault in southwestern Utah—Paleoseismology of Utah Volume 14: Utah Geological Survey Special Study 119, 81 p.

Lund, W.R., Knudsen, T.R., Sharrow, D.L., 2010, geologic hazards of the Zion National Park Geologic-Hazard Study Area, Washington and Kane Counties, Utah, Utah Geological Survey, Special Study Map SS-133, 97 p,

McDougall, S., Hungr, O., 2006, Landslide dynamic analysis in 2D and 3D, Sea to Sky Geotechnique, the 59th Canadian Geotechnical Conference, Vancouver, 2006, 5 p.

McDougall, S., Mckinnon, M., Hungr, O., 2012, Developments in landslide runout, in Landslides: Types, Mechanisms and Modeling, J.J. Clague and D. Stead, editors, Cambridge University, Cambridge England, Cambridge University Press, pp. 187-195.

National Park Service (NPS), 2014, Annual Park Recreation Visitation (1904 - Last Calendar Year), online resource accessed September 26, 2014, https://irma.nps.gov/.

Nagelisen, J., Moore, J.R., Vockenhuber, C., Ivy-Ochs, S., 2015, Post-glacial rock avalanches in the Obersee Valley, Glarner Alps, Switzerland, Geomorphology vol. 238, pp. 94-111.

Pankow, K.L., Moore, J.R., Hale, J.M., Koper, K.D., Kubacki, T., Whidden, K.M., McCarter, M.K., 2014, Massive landslide at Utah copper mine generates wealth of geophysical data, GSA Today, vol. 24, no. 1, pp. 4-9, doi:10.1130/GSATG191A.1.

Pipiringos, G.N., O'Sullivan, R.B., 1978, Principal unconformities in Triassic and Jurassic rocks, Western Interior United States—A preliminary survey, Geological Survey Professional Paper 1035-A, 29 p.

Pirulli, M., 2009, The Thurwieser rock avalanche (Italian Alps): Description and dynamic analysis, Engineering Geology, vol. 109, p. 89-92.

Pirulli, M., Mangeney, A., 2008, Results of back-analysis of the propagation of rock avalanches as a function of the assumed rheology, Rock Mechanics and Rock Engineering, vol. 41 no. 1, p. 59-84.

Reiche, P., 1937, The toreva-block: A distinctive landslide type, The Journal of Geology, vol. 45, no. 5, pp. 538-548.

Rogers, C.M., Engelder, T., 2004, The feedback between joint-zone development and downward erosion of regularly spaced canyons in the Navajo Sandstone, Zion National Park, Utah, in The initiation, propagation, and arrest of joints and other fractures, Cosgrove, J.W., and Engelder, T., editors, Geological Society, London, Special Publications, vol. 231, p. 49-71.

Schuster, R. L., Wieczorek, G.F., 1995, Reconnaissance of the April 12, 1995 Landslide in Zion Canyon, Zion National Park, Utah. U.S. Geological Survey, Branch of Earthquake and Landslide Hazards, Administrative Report dated May 2, 1995. 19p.

Sharrow, D., 2012, Summary of the Sentinel Slide Project, Zion National Park, unpublished manuscript.

Solomon, B.J., 1995, Geologic reconnaissance of the Zion Canyon landslide of April 12, 1995, Zion National Park, Washington County, Utah, in Technical reports for 1994 – 1995 applied geology program, compiled by B.H. Mayes, Utah Geological Survey Report of Investigation 228, p. 74-79.

Sosio, R., Crosta, G.B., Hungr, O., 2008, Complete dynamic modelling calibration for the Thurwieser rock avalanche (Italian Central Alps), Engineering Geology, vol. 100, no. 1-2, p. 11-26.

Stock, G.M., Uhrhammer, R.A., 2010, Catastrophic rock avalanche 3600 years BP from El Capitan, Yosemite Valley, California, Earth Surface Processes and Landforms, vol. 35, pp. 941-951, doi: 10.1002/esp.1982.

Stone, J.O., 2000, Air pressure and cosmogenic isotope production, Journal of Geophysical Research, vol. 105, v. B10 23 p.

Taylor, T., 2008, Images of America Zion National Park, Charleston, SC, Chicago IL, Portsmouth NH, San Francisco CA, Arcadia Publishing, 129 p.